A Distributed Networked Approach for Fault Detection of Large-Scale Systems

Francesca Boem, Riccardo M. G. Ferrari, Christodoulos Keliris, *Member, IEEE*, Thomas Parisini, *Fellow, IEEE*, and Marios M. Polycarpou, *Fellow, IEEE*

***Abstract*—Networked systems present some key new challenges in the development of fault-diagnosis architectures. This paper proposes a novel distributed networked fault detection methodology for large-scale interconnected systems. The proposed formulation incorporates a synchronization methodology with a filtering approach in order to reduce the effect of measurement noise and time delays on the fault detection performance. The proposed approach allows the monitoring of multirate systems, where asynchronous and delayed measurements are available. This is achieved through the development of a virtual sensor scheme with a model-based resynchronization algorithm and a delay compensation strategy for distributed fault–diagnostic units. The monitoring architecture exploits an adaptive approximator with learning capabilities for handling uncertainties in the interconnection dynamics. A consensus-based estimator with time-varying weights is introduced, for improving fault detectability in the case of variables shared among more than one subsystem. Furthermore, time-varying threshold functions are designed to prevent false-positive alarms. Analytical fault detectability sufficient conditions are derived, and extensive simulation results are presented to illustrate the effectiveness of the distributed fault detection technique.**

***Index Terms*—Distributed systems, fault detection, large-scale systems, networked control systems.**

I. Introduction and State of the Art

THE growing scientific interest for networked and distributed systems is evident by the large number of works cited in surveys and books (see, for example, [1], [2]). As complexity and interconnectedness increase, there is a higher risk of faulty operation in one or more components/subsystems of the overall system. In the presence of such faulty scenarios, it is difficult to detect and isolate the fault, as well as to design methods for bringing the system back to normal operation. Faults in a low-level component may have a manageable impact on system operation; on the other hand, high-level faults can have significant consequences (for example, human safety, major economic effects, and environmental impact) if not detected and handled promptly. Therefore, there is a need to develop fault detection tools in the context of large-scale, distributed, and networked systems, which is the aim of this paper.

Recently there has been a growing interest toward distributed architectures for the monitoring of large-scale and/or networked systems (see [3]–[14]). For instance, some recent works on monitoring and diagnosis of Cyber Physical Systems (CPSs) deal with the detection of attacks against process control systems [15] and cyberphysical attacks in power networks [16]–[19]. In [20] and [21] distributed schemes to detect and isolate the attacks on networked control systems using observers are developed. In [21], applications to power networks and robotic formations are presented. All these works about cyber-attacks consider linear system models. Another research topic that has attracted significant interest recently is the design of fault detection methods for multiagent systems (see as example [22]–[24]).

In this paper, the distributed fault-diagnosis approach presented in [4] and [5] for nonlinear systems is generalized to address issues emerging when considering networked diagnosis systems. In particular, when dealing with communication networks, one of the main issues is the presence of delays and packet dropouts that degrade performance and could be a source of instability, misdetection, and false alarms. Delays and packet losses in the communication networks are dealt with in this paper. While there is an extensive literature addressing this issue in the control framework (see, for example, [25]–[29], and the references cited therein), much less literature is available in the case of fault diagnosis, especially for large-scale systems. In particular, only the decentralized fault-diagnosis problem is considered (see, for example, [30]–[33], in which fault detection and isolation schemes for networked systems are addressed). An exception is [34] and the references cited therein, dealing with discrete-event systems. Despite these results, the design of fault-diagnosis schemes specifically for distributed and large-scale systems is still a challenging task, and the issues deriving from networked architectures are not taken into account. Some works consider the problem of monitoring networked control systems, where delays and packet dropouts are induced in

Manuscript accepted February 16, 2016. This work was supported in part by the Engineering and Physical Sciences Research Council under the STABLE-NET grant EP/L014343/1, by the European Research Council under the Fault-Adaptive ERC Advanced Grant 291508, and by the European Union AMBI FP7-PEOPLE grant 324432. Recommended by Associate Editor C. Seatzu.

F. Boem is with the Department of Electrical and Electronic Engineering, Imperial College London, London SW7 2AZ, U.K. (e-mail: f.boem@imperial.ac.uk).

R. M. G. Ferrari is with the Delft Center for Systems and Control, Delft University of Technology, 2628 CD Delft, The Netherlands (e-mail: r.ferrari@tudelft.nl).

C. Keliris and M. M. Polycarpou are with the KIOS Research Center for Intelligent Systems and Networks, Department of Electrical and Computer Engineering, University of Cyprus, Nicosia 1678, Cyprus (e-mail: keliris.chris@gmail.com; mpolycar@ucy.ac.cy).

T. Parisini is with the Department of Electrical and Electronic Engineering, Imperial College London, London SW7 2AZ, U.K., and with the Department of Engineering and Architecture, University of Trieste, 34127 Trieste, Italy (e-mail: t.parisini@gmail.com).

the communication between controller, actuators and sensors [35], [36]. Instead, here we consider distributed fault detection architectures. Moreover, dealing with a networked architecture, the possibility to have multirate systems and asynchronous measurements is considered. Also in this case, while the literature addressing this topic in the control field is increasing (see [37] and [38] as example), in the distributed fault diagnosis these issues still have not been addressed (see [39] for the centralized case).

In the following we provide the main aspects of the problem formulation, the research objectives and the proposed methodology.

A. Problem Formulation

In previous works, a distributed approach to fault diagnosis (FD) for large-scale systems has been developed, both in the continuous-time [4] and in the discrete-time [5] frameworks. In the following, a brief summary of this methodology is given for the readers' convenience and for the sake of completeness. Details can be found in [4] and [5]. The limitations of the existing monitoring architectures in networked scenarios in terms of detectability are illustrated, and some solutions are presented.

A nonlinear uncertain large-scale system, composed of N interconnected subsystems, is considered. Its monolithic model is described by

$$\dot{x}(t) = f\left(x(t), u(t)\right) + \eta\left(x(t), u(t)\right) + \phi\left(x(t), u(t), t\right) \quad (1)$$

where $x \in \mathbb{R}^{n^x}$ and $u \in \mathbb{R}^{n^u}$ are the state and the control input of the system, respectively, $f : \mathbb{R}^{n^x} \times \mathbb{R}^{n^u} \mapsto \mathbb{R}^{n^x}$ models the nominal dynamics, $\eta : \mathbb{R}^{n^x} \times \mathbb{R}^{n^u} \mapsto \mathbb{R}^{n^x}$ represents the modeling uncertainty, and $\phi : \mathbb{R}^{n^x} \times \mathbb{R}^{n^u} \times \mathbb{R} \mapsto \mathbb{R}^{n^x}$ describes the effects on system dynamics due to any deviation from the nominal model, which take place for $t \geq T_0$, where T_0 denotes the unknown fault occurrence time (i.e., $\phi(x(t), u(t), t) = 0$, for $t < T_0$). The following well-posedness assumption is needed.

Assumption 1: The state variables x and control variables u are uniformly bounded before and after the occurrence of a fault, that is, there exists a compact region $\mathcal{R} \subset \mathbb{R}^{n^x} \times \mathbb{R}^{n^u}$ such that $(x(t), u(t)) \in \mathcal{R}$, $\forall\, t \geq 0$. □

The state variables are measured by n^y sensors, whose outputs are described by the following equation:

$$m(t) = Gx(t) + w(t) \quad (2)$$

where $m \in \mathbb{R}^{n^y}$ is a vector collecting the measurements of the components of the state vector x, $w \in \mathbb{R}^{n^y}$ denotes the vector of the measurement noise, and G is a full-rank $n^y \times n^x$ matrix having one single element equal to 1 for each row, representing the state component measured by each sensor. We assume that each state component is measured at least by one sensor, that is, $n^y \geq n^x$. It is worth noting that—under suitable additional assumptions (see [6] and [40])—the generalization to the input/output case could be carried out, but this is outside the scope of this paper.

Assumption 2: For each ith measurement $m^{(i)}$, with $i = 1, \ldots, n^y$ being the vector component index, the measurement uncertainty term $w^{(i)}$ is an unstructured and unknown function of time, but it is bounded by a known positive time-function $\bar{w}^{(i)}(t)$ such that $|w^{(i)}(t)| \leq \bar{w}^{(i)}(t)$, $i = 1, \ldots, n^y$, $t \geq 0$. □

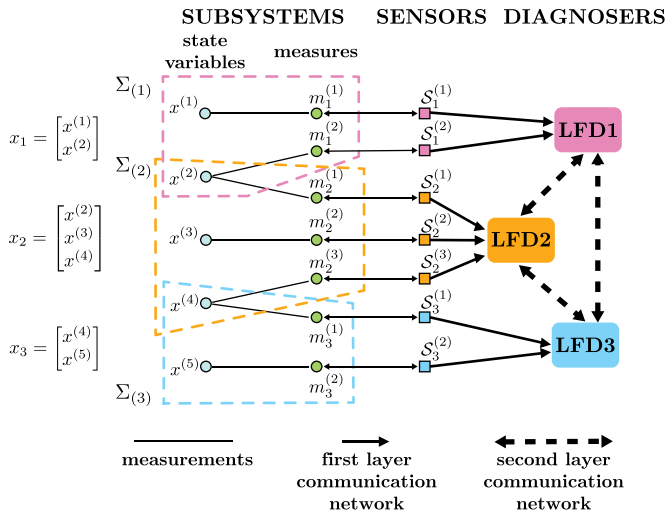

Fig. 1. Example of the proposed multilayer fault detection architecture. The system state variables (represented by light blue circles on the left) are measured by the sensor layer (center). The measurements are represented by green circles, while the actual sensors by small squares. Each subsystem (colored dotted boundaries) is described by its local variables and its local measurements. The sensors communicate their measurements to the LFDs by means of the first-level communication network. The second-level communication network (right) allows the diagnosers to communicate with each other exchanging information.

As illustrated in [4] and [5], a structural graph can be associated with system (1), and a formal (possibly overlapping) decomposition of the graph can be defined to identify N subsystems. More specifically, in case that more than one sensor is available to measure a given state variable $x^{(i)}$, it might be useful to devise a decomposition with overlapping subsystems such that the variable $x^{(i)}$ is "shared" among these subsystems and each sensor measuring $x^{(i)}$ belongs to a different subsystem (see left side of Fig. 1). In this paper, we are not dealing with the problem of finding an optimal way of decomposing the system (see [41]); hence, the decomposition is assumed to be known *a priori*. Moreover, we assume that the existing decomposition implies the allocation of the sensors: each nonshared variable is measured exactly by one sensor; shared variables are measured by a number of sensors equal to the number of sharing subsystems. Each sensor is allocated to one subsystem.

The Ith subsystem Σ_I is modeled as

$$\Sigma_I : \dot{x}_I(t) = f_I\left(x_I(t), u_I(t)\right) + g_I\left(x_I(t), z_I(t), u_I(t)\right) + \phi_I\left(x_I(t), z_I(t), u_I(t), t\right) \quad (3)$$

where $x_I \in \mathbb{R}^{n_I^x}$ and $u_I \in \mathbb{R}^{n_I^u}$ are the local state and control input vectors, and $z_I \in \mathbb{R}^{q_I}$ is the vector of the interconnection variables, which are state variables of neighboring subsystems that influence the Ith subsystem. The function $g_I : \mathbb{R}^{n_I^x} \times \mathbb{R}^{q_I} \times \mathbb{R}^{n_I^u} \mapsto \mathbb{R}^{n_I^x}$ represents the uncertain interconnection between subsystems, considering also the local effects of the modeling uncertainty function η, $f_I : \mathbb{R}^{n_I^x} \times \mathbb{R}^{n_I^u} \mapsto \mathbb{R}^{n_I^x}$ models the local nominal healthy behavior. Finally, $\phi_I : \mathbb{R}^{n_I^x} \times \mathbb{R}^{q_I} \times \mathbb{R}^{n_I^u} \times \mathbb{R} \mapsto \mathbb{R}^{n_I^x}$ describes the local fault effects. In this paper, we consider both process and actuator faults.

Each sensor is associated with exactly one subsystem (see Fig. 1). The *local sensor* $S_I^{(i)}$ associated with the Ith subsystem provides a measurement $m_I^{(i)}$ of the ith component of the local

state vector x_I according to the output equation

$$S_I^{(i)} : m_I^{(i)}(t) = x_I^{(i)}(t) + w_I^{(i)}(t), \quad i = 1, \ldots, n^{x_I} \qquad (4)$$

where $w_I^{(i)}$ denotes the noise affecting the ith sensor of the Ith subsystem. It is worth noting that in the local model output (4), there is a correspondence between sensors and state variables, while this may be not true in the global model (2), since more than one sensor may measure the same variable (see again Fig. 1). We assume that the control input is available without any error or delay.

Similarly to [5], each subsystem of the above decomposition is monitored by a specific local fault diagnoser (LFD). Each LFD receives from its local sensors the noisy state measurements forming the vector $m_I = \text{col}(m_I^{(i)}, i = 1, \ldots, n^{x_I})$ [see (4)] and, from the Jth neighboring LFD the noisy measurements $m_{z_I}^{(i)}$, $i = 1, \ldots, q_I$ of the local state variables components $x_J^{(i)}$ that influence the Ith subsystem (i.e., the variables $x_J^{(i)}$ belonging to the interconnection vector z_I).

Each LFD computes a local state estimate $\hat{x}_I(t)$ based on the local Ith model, by communicating the interconnection variables (and possibly other information) to neighboring LFDs. The state estimator takes on a different structure depending on whether the specific ith component $x^{(i)}$ of the state is shared among more than one subsystem or not. In the former case, a deterministic consensus procedure is designed to take advantage of the availability of more than one sensor measuring the same variable [4], [5].

The LFD implements a model-based fault detection method: the local estimation error $\epsilon_I(t) = m_I(t) - \hat{x}_I(t)$ is compared, component-by-component, to a time-varying threshold $\bar{\epsilon}_I(t)$, suitably computed in order to guarantee the absence of false alarms. Moreover, a filtering design [42] is introduced to reduce the conservativeness of the detection thresholds, which is here adapted in the current formulation under discrete time.

B. Objectives and Contributions

The existing approaches for distributed fault diagnosis of nonlinear uncertain large-scale systems that we have previously described are based on some underlying assumptions that may restrict their applicability, namely:

1) *global synchronization:* subsystems, sensors, and LFDs are assumed to share the same clock and sampling frequency;
2) *perfect information exchange:* it is assumed that information exchanged between LFDs and communicated from the system to the LFDs is without any error nor delay, and it is immediately available at any point of the diagnosis system.

In several realistic contexts, 1) and 2) may not hold, and as a consequence: i) some faults may become undetectable due to the fact that LFDs make detection decisions based on outdated information; ii) delays in information exchange may cause longer detection times; and iii) the lack of accurate and timely information may cause false alarms.

In this paper, the distributed fault-diagnosis methodology presented in [4] and [5] is extended to address the above-mentioned limitations. More specifically:

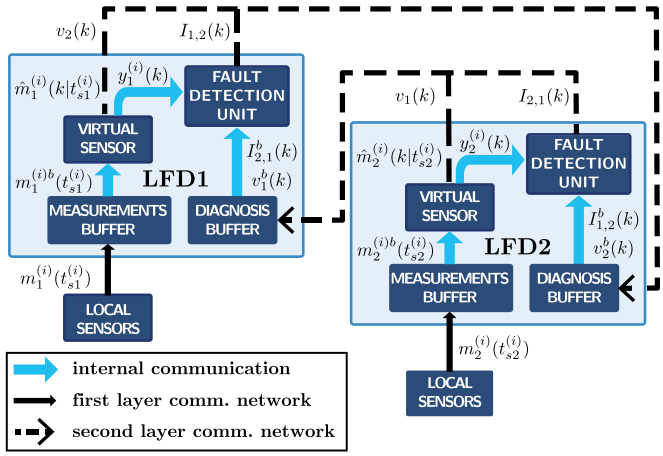

Fig. 2. Example of a two-LFD architecture. The internal structure of each LFD is shown, composed of two buffers (the measurements buffer and the diagnosis buffer) to collect the information received, respectively, by the local sensors and neighboring LFDs, the Virtual Sensor (processing the received measurements), and the Fault Detection unit, responsible for the monitoring analysis. The communicated information between LFDs is represented.

a) a multilayer distributed fault-diagnosis architecture is proposed consisting of three layers (the system layer, the sensor layer, and the diagnosis level; see Fig. 1); this facilitates the investigation of the relationships between the different elements that compose networked systems;
b) a delay compensation strategy is devised to address delays and packet losses in the communication network between the LFDs (see [43] for some preliminary results) using timestamps and a buffer, called *diagnosis buffer* (see Fig. 2);
c) a model-based resynchronization algorithm is embedded in the diagnosis procedure; this algorithm is based on *virtual sensors* implemented in the LFDs and on the use of a *measurements buffer* (see Fig. 2);
d) the filtering-based design recently proposed in [9] and [42] is modified and integrated into the proposed distributed fault-diagnosis methodology thus enhancing fault detection robustness and facilitating less conservative conditions for fault-detectability.

In Fig. 2, an example of a two LFDs architecture is presented to provide more insight into the structure of the proposed scheme.

The paper is organized as follows. In Section II, the distributed fault detection architecture is described enhancing the presence of a *physical* system (which is being diagnosed for faults), of the sensors (which are made of a *physical* part interacting with the system to be diagnosed) and of a *computational* (cyber) part able to take process measurements and exchange information with other sensors of the network to synchronize with each other) and of the local diagnosers (which are *computational*-systems as well and able to make model-based estimation and exchange information with each other). In Section IV, the distributed fault detection algorithm is presented also detailing the resynchronization scheme, the time-varying consensus mechanism, and the delay compensation strategy. In Section V sufficient conditions for fault detectability are presented that characterize the class of detectable faults, and

in Section VI simulation results illustrating the effectiveness of the fault-diagnosis scheme are presented. Finally, Section VII reports some concluding remarks.

II. Three-Layer Fault-Diagnosis Architecture

The proposed distributed fault-detection architecture is made of three layers: the system layer, the sensor layer, and the diagnosis layer. In Fig. 1, this layout is shown in a pictorial way. These three layers are briefly described next.

The *system layer* refers to the large-scale system to be monitored. It is described by the continuous-time state (1) and the output (2).

The *sensor layer* consists of the available sensors taking measurements $m_I^{(i)}(t)$ in continuous-time [see (4)] and sampling and sending such measurements to the Ith LFD at time instants $t_{sI}^{(i)}$ that are not necessarily equally spaced in time. As we do not assume that the measurements delivered by the sensors are synchronized with each other, each measurement is labeled with a timestamp (TS) [44] to indicate the time instant $t_{sI}^{(i)}$ at which the measurements are taken by sensor $S_I^{(i)}$ in the time coordinate t.

The communication between the sensors and the LFDs is achieved through the *first-level communication network* (see Fig. 1). This network can introduce delays and packet losses, for instance because of collision between different sensors trying to communicate at the same time. Therefore, measurements communicated from the sensors to LFDs may be received at any time instant.

The *diagnosis layer* consists of the previously introduced LFDs providing a distributed fault-diagnosis procedure. The structure of each LFD is shown in Fig. 2. As previously mentioned, each LFD receives the measurements from specific sensors with the aim to provide local fault-diagnosis decisions. The LFDs operate in a discrete-time synchronous time frame $k \in \mathbb{Z}$ which turns out to be more convenient for handling any communications delays, as will be seen in the next sections. For the sake of simplicity, the sampling time of the discrete time frame is assumed to be unitary and the reference time is common, that is, the origin of the discrete-time axis is the same as that of the continuous-time axis. Therefore, the operation of the LFDs is based on the local discrete-time models, which are the discrete-time version of local models (3)

$$x_I(k+1) = f_I\left(x_I(k), u_I(k)\right) + g_I\left(x_I(k), z_I(k), u_I(k)\right) + \phi_I\left(x_I(k), z_I(k), u_I(k), k\right) \quad (5)$$

where ϕ_I describes the local discretized fault effects, occurring at some discrete-time k_0 (that is, $\phi_I(x_I(k), z_I(k), u_I(k), k) = 0, k < k_0$). Each LFD exchanges information with neighboring LFDs by means of the *second-level communication network* (see right side of Figs. 1 and 2). As we will see in the following, the exchanged information consists in the resynchronized interconnection variables v_J and a vector that we denote $I_{I,J}$, collecting some variables needed for fault detection purposes in the case of shared variables (as will be explained in Section IV).

In summary, two different and not reliable communication networks are considered in this paper: the first-level communication network allows each LFD to communicate with its local sensors, and the second-level communication network allows the communication between different LFDs for detection purposes. Both these communication networks may be subject to delays and packet losses. Given the different nature of the networks (the first is local, while the second is connecting different subsystems, which may be geographically apart), in the next section we provide two different strategies to manage communication issues: a resynchronization method for the first-level communication network and a delay compensation strategy for the second-level communication network.

III. Resynchronization at Diagnosis Level

Let us consider a state variable $x_I^{(i)}(t)$; as mentioned before, at time $t = t_{sI}^{(i)}$ the sensor $S_I^{(i)}$ takes the measurement $m_I^{(i)}(t_{sI}^{(i)})$ and sends it to the Ith LFD with a timestamp $t_{sI}^{(i)}$. The Ith diagnoser receives the measurement sent by $S_I^{(i)}$ at time $t_{aI}^{(i)} > t_{sI}^{(i)}$. Since the LFDs run the distributed fault-diagnosis algorithm with respect to a discrete-time framework associated with an integer k [see (5)], an online resynchronization procedure has to be carried out at the diagnosis level. Moreover, the possible time-varying delays and packet losses introduced by the communication networks between the local sensors and the corresponding LFDs have to be addressed, since they may affect the fault-diagnosis decision. Note that the classical discrete-time FD architecture assumes that quantities sampled at exactly time k are used to compute quantities related to time $k+1$. Unfortunately, the LFDs may receive measurements associated with time instants different from k, because of transmission delays and because of the arbitrary sampling time instants of the sensors. The availability of the timestamp $t_{sI}^{(i)}$ enables each LFD to implement a set of *local virtual sensors* by which the resynchronization of the measurements received at the diagnosis level is implemented. We assume that sensors and diagnosers share the same clock at the local level.[1]

Specifically, each LFD collects the most recent sensors measurements in a buffer and computes a projection $\hat{m}_I^{(i)}(k|t_{sI}^{(i)})$ of these latest available measurements $m_I^{(i)}(t_{sI}^{(i)})$, $i = 1, \ldots, n_I^x$, to the discrete time instant[2] $k \geq t_{aI}^{(i)} > t_{sI}^{(i)}$, by integrating the local nominal model on the time interval $[t_{sI}^{(i)}, k]$.

Remark 1: Let us note that measurements may be related to and could be received also before time $k-1$, without any assumption on the delay length, thus allowing the presence of measurements packets losses. Moreover, thanks to the use of the timestamps and the buffers, "out-of-sequence" packets can be managed. The same measurement could be used by the virtual sensor more than once to obtain more than one projections related to different discrete time instants.

[1] As example, this could be obtained in accordance with the IEEE 1588-2002 standard ("Standard for a Precision Clock Synchronization Protocol for Networked Measurement and Control Systems"), where each diagnoser can be selected as a synchronization master for the sensors that communicate with it.

[2] Recall that the sampling time of the diagnosers is supposed to be unitary for simplicity.

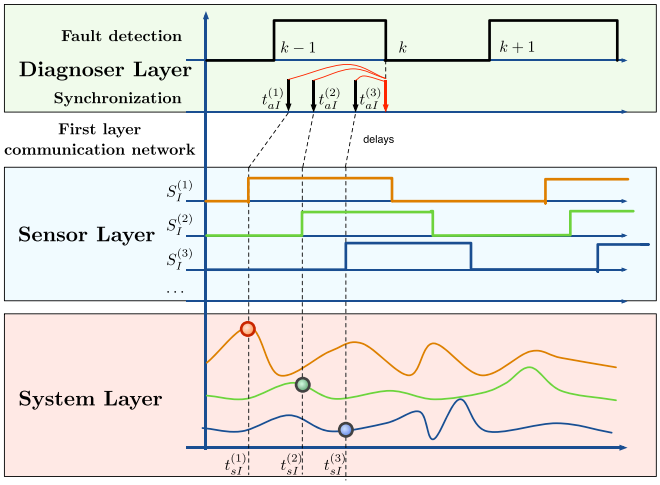

Fig. 3. Resynchronization procedure needed to manage delays and packet losses in the communication networks between each LFD and its local sensors. A single LFD is considered whose local model depends on three variables, which are measured by three different sensors. The clock signals of each layer involved are shown.

The projected measurement $\hat{m}_I^{(i)}(k|t_{sI}^{(i)})$ can be computed by noticing that, *under healthy mode of behavior*, the local nominal model (3) for the state component i at any time $t > t_{sI}^{(i)}$ can be rewritten as

$$x_I^{(i)}(t) = x_I^{(i)}\left(t_{sI}^{(i)}\right) + \int_{t_{sI}^{(i)}}^{t} \Big[f_I^{(i)}\left(x_I(\tau), u_I(\tau)\right) + g_I^{(i)}\left(x_I(\tau), z_I(\tau), u_I(\tau)\right)\Big] d\tau.$$

Hence, the LFD implements a *virtual sensor* that generates an estimate of the measurement at discrete-time k given by

$$\hat{m}_I^{(i)}\left(k\middle|t_{sI}^{(i)}\right) = m_I^{(i)}\left(t_{sI}^{(i)}\right) + \int_{t_{sI}^{(i)}}^{k} \Big[f_I^{(i)}\left(\hat{m}_I\left(\tau\middle|t_{sI}^{(i)}\right), u_I(\tau)\right) + \hat{g}_I^{(i)}\left(\hat{m}_I\left(\tau\middle|t_{sI}^{(i)}\right), \hat{m}_{zI}\left(\tau\middle|t_{sI}^{(i)}\right), u_I(\tau)\right)\Big] d\tau \quad (6)$$

where $\hat{g}_I$ characterizes an adaptive approximator designed to learn the unknown interconnection function g_I [45] and $\hat{m}_{zI}$ are the projections of the measured interconnection variables m_{zI}. An example enhancing the resynchronization procedure for one LFD monitoring a subsystem with three state variables is illustrated in Fig. 3.

Remark 2: It is worth noting that the discrete-time index $k \in \mathbb{Z}$ represents kind of a "virtual timestamp" (vTS) computed by the LFDs after the resynchronization task and communicated in the second-level communication network between LFDs. This will be exploited in Section IV.

Remark 3: Although in (6), for analysis purposes, $\hat{g}_I$ represents the output of a continuous-time adaptive approximator, for implementation reasons, a suitable discrete-time approximator will be used, designed as explained in Section IV-B.

The above-described projection and resynchronization procedure gives rise to an additional source of measurement uncertainty: the *virtual measurement error*, which is defined as

$$\xi_I^{(i)}(k) \triangleq \hat{m}_I^{(i)}\left(k\middle|t_{sI}^{(i)}\right) - x_I^{(i)}(k).$$

For the sake of analysis, it is worth noting that, due to synchronization and measurement noise, the virtual measurement error is given by

$$\begin{aligned}\xi_I^{(i)}(k) &= m_I^{(i)}\left(t_{sI}^{(i)}\right) - x_I^{(i)}\left(t_{sI}^{(i)}\right) \\ &\quad + \int_{t_{sI}^{(i)}}^{k} \left[\Delta_{\text{synch}} f_I^{(i)}(\tau) + \Delta_{\text{synch}} g_I^{(i)}(\tau)\right] d\tau \\ &= w_I^{(i)}\left(t_{sI}^{(i)}\right) + \int_{t_{sI}^{(i)}}^{k} \left[\Delta_{\text{synch}} f_I^{(i)}(\tau) + \Delta_{\text{synch}} g_I^{(i)}(\tau)\right] d\tau \quad (7)\end{aligned}$$

where

$$\Delta_{\text{synch}} f_I^{(i)}(\tau) \triangleq f_I^{(i)}\left(\hat{m}_I\left(\tau\middle|t_{sI}^{(i)}\right), u_I(\tau)\right) - f_I^{(i)}(x_I(\tau), u_I(\tau))$$

$$\Delta_{\text{synch}} g_I^{(i)}(\tau) \triangleq \hat{g}_I^{(i)}\left(\hat{m}_I\left(\tau\middle|t_{sI}^{(i)}\right), \hat{m}_{zI}\left(\tau\middle|t_{sI}^{(i)}\right), u_I(\tau)\right) - g_I^{(i)}\left(x_I(\tau), z_I(\tau), u_I(\tau)\right).$$

For notational convenience, we now collect the projected measurements $\hat{m}_I^{(i)}(k|t_{sI}^{(i)})$ in a vector, which, in the following, we denote as $y_I(k)$, with k being its vTS:

$$y_I(k) = \text{col}\left\{\hat{m}_I^{(i)}\left(k\middle|t_{sI}^{(i)}\right), i = 1, \ldots, n_I^x\right\}.$$

Therefore, it is as if the virtual sensor implemented by the LFDs takes uncertain local measurements y_I of the state x_I, according to

$$y_I(k) = x_I(k) + \xi_I(k)$$

where ξ_I is the unknown virtual measurement error (7). Moreover, in place of the interconnection variables z, only the vector

$$v_I(k) = z_I(k) + \varsigma_I(k)$$

is available for diagnosis, where ς_I is composed by the components of ξ_J affecting the relevant components of y_J (as before, J refers to a neighboring subsystem). For simplicity, we assume here that the control signal u_I is available to the diagnoser without any delays or other uncertainty.

The virtual measuring errors ξ_I and ς_I are unstructured and unknown. For fault detection, it is not necessary to compute them, but, for each $i = 1, \ldots, n_I^x$ and $h = 1, \ldots, q_I$, it is possible to compute a bound for their components using (7)

$$\left|\xi_I^{(i)}(k)\right| \le \bar{\xi}_I^{(i)}(k), \qquad \left|\varsigma_I^{(h)}(k)\right| \le \bar{\varsigma}_I^{(h)}(k)$$

where

$$\bar{\xi}_I^{(i)}(k) = \bar{w}_I^{(i)}\left(t_{sI}^{(i)}\right) + \int_{t_{sI}^{(i)}}^{k} \bar{\Delta}_{\text{synch}} f_I^{(i)}(\tau) + \bar{\Delta}_{\text{synch}} g_I^{(i)}(\tau) d\tau \quad (8)$$

is a positive function and $\bar{w}_I^{(i)}$ is the one defined in Assumption 2. Moreover:

$$\bar{\Delta}_{\text{synch}} f_I^{(i)}(\tau) = \max_{x_I \in \mathcal{R}^{x_I}} \left| f_I^{(i)}(\hat{m}_I(\tau), u_I(\tau)) - f_I^{(i)}(x_I(\tau), u_I(\tau)) \right|$$

remembering that the set $\mathcal{R}^{x_I}$ is the domain of the state, and $\bar{\Delta}_{\text{synch}} g_I^{(i)}(\tau)$ can be computed in an analogous way as in (31)

(see Section IV-D). The bound $\bar{\varsigma}_I$ is computed with the same procedure by the neighboring subsystems. In the next section, the fault-diagnosis procedure is presented.

IV. Distributed Fault Detection Methodology

For fault detection purposes, each LFD communicates with neighboring LFDs. It is assumed that the inter-LFD communication is carried over a packet-switched network, which we call the *second-level communication network*, possibly subject to packet delays and losses. In order to manage delays in this network, the data packets are timestamped, with the virtual timestamp, which contains the time instant the virtual measurements are referred to. In this layer, we assume to have perfect clock synchronization between the LFDs. In this way, all the devices of the monitoring architecture can share the same clock, that is, they know the reference time, and the use of timestamps can be valid.

Furthermore, we propose to provide each LFD with a buffer to collect the variables sent by neighbors. In the following, we denote with the superscript "b" the most recent value of a variable (or of a communicated function value) in the corresponding buffer of a given LFD; for example, v_I^b denotes the most recent value of the measured interconnection vector v_I contained in the buffer of the Ith LFD, while $[f_I(\cdot)]^b$ denotes the most recent value of the function $[f_I(\cdot)]$ in the buffer.

Each LFD computes a nonlinear adaptive estimate $\tilde{x}_I$ of the associated monitored subsystem state x_I. The local estimator, called *fault detection approximation estimator* (FDAE), is based on the local discrete-time nominal model (5). In this paper, differently from [5], to dampen the effect of the virtual measurement error $\xi_I(k)$, each measured variable $y_I^{(i)} = x_I^{(i)} + \xi_I^{(i)}$ is filtered by $H(z)$, where $H(z)$ is a pth order, asymptotically stable filter with proper transfer function

$$H(z) = \frac{z(d_1 z^{-1} + d_2 z^{-2} + \cdots + d_p z^{-p})}{c_0 + c_1 z^{-1} + \cdots + c_p z^{-p}}. \tag{9}$$

Generally, each measured variable $y_I^{(i)}(k)$ can be filtered by a different filter with the exception of shared variables where for each shared variable the same filters must be used. In this paper, without loss of generality, we consider $H(z)$ to be the same for all the output variables, in order to simplify notation and presentation. The filter $H(z)$ can be written as $H(z) = zH_p(z)$. The filters $H(z)$ and $H_p(z)$ (with impulse responses $h(k)$ and $h_p(k)$ respectively) are asymptotically stable and hence BIBO stable. Therefore, for bounded virtual measurement error $\xi_I(k)$, the filtered virtual measurement error[3] $\Xi_I(k) \triangleq H(z)[\xi_I(k)]$ is bounded as follows:

$$\left|\Xi_I^{(i)}(k)\right| \leq \bar{\Xi}_I^{(i)}(k) \quad i = 1, \ldots, n_I^x \tag{10}$$

where $\bar{\Xi}_I^{(i)}$ are bounding functions that can be computed as $\bar{\Xi}_I^{(i)} \triangleq \bar{H}(z)[\bar{\xi}_I^{(i)}]$, being $\bar{H}(z)$ a filter with impulse response $\bar{h}(k) = |h(k)|$ and using (8). Note that we denote with capital letters the filtered signals.

[3]For notational convenience, in the paper we use the shorthand $H(z)[\xi(k)]$ to denote $\mathcal{Z}^{-1}\{H(z)\Xi(z)\}$.

A. Fault Detection Estimation and Residual Generation

In this subsection we present a method for computing the local state estimate $\tilde{x}_I$ for fault detection purposes. In the case of a nonshared state component i, the local estimation $\tilde{x}_I^{(i)}$ is given by

$$\tilde{x}_I^{(i)}(k+1) = f_I^{(i)}\left(y_I(k), u_I(k)\right) + \hat{g}_I^{(i)}\left(y_I(k), v_I^b(k), u_I(k), \hat{\vartheta}_I(k)\right) \tag{11}$$

where $\hat{g}_I$ is the output of an adaptive approximator designed in Section IV-B to learn the unknown interconnection function g_I, $\hat{\vartheta}_I \in \hat{\Theta}_I$ denotes its adjustable parameters vector, and t_b is the virtual timestamp of the most recent information received v_I^b in the buffer at time k.

In the case that a state variable $x^{(s)}$ of the global model (1) is shared among more than one LFD $J \in \mathcal{O}_s$ (being $\mathcal{O}_s$ the set of the subsystems sharing $x^{(s)}$), the estimation can be computed using a consensus approach (see [5]). We denote with s_J the local index of the global variable s, that is[4] $x^{(s)} = x_J^{(s_J)}$, $\forall\, J \in \mathcal{O}_s$. For the Ith subsystem, the local estimation $\tilde{x}_I^{(s_I)}$ is given by

$$\tilde{x}_I^{(s_I)}(k+1) = \sum_{J \in \mathcal{O}_s} W_s^{(I,J)} \Big[f_J^{(s_J)}\left(y_J(k), u_J(k)\right) + \hat{g}_J^{(s_J)}\left(y_J(k), v_J^b(k), u_J(k), \hat{\vartheta}_J(k)\right) \Big]^b \tag{12}$$

with initial condition $\tilde{x}_I^{(s_I)}(0) = y_I^{(s_I)}(0)$. Each Jth LFD communicates to neighboring LFDs sharing variable s the local value of the function $f_J^{(s_J)}(y_J(k), u_J(k)) + \hat{g}_J^{(s_J)}(y_J(k), v_J^b(k), u_J(k), \hat{\vartheta}_J(k))$ (this consists in the first part of vector $I_{I,J}$, together with some information needed to compute the thresholds). In this way, it is not necessary for the local diagnosers to know the other subsystems models. The terms $W_s^{(I,J)}$ are the components of a stochastic matrix W_s (the values of each row add up to 1). In Section IV-E, the definition of the weight matrix W_s in order to improve detectability capabilities is given. It is worth noting that the formulation of (12) includes the case of a nonshared variable component i [see (11)], since, in this case $\mathcal{O}_i = \{I\}$ and hence index J is simply equivalent to I, with $W_i^{(I,I)} = 1$, by definition.

We now explain the residual generation: the local estimation residual error $r_I(k)$ is defined as

$$r_I(k) \triangleq Y_I(k) - \widehat{Y}_I(k) \tag{13}$$

where we obtain the filtered output $Y_I(k)$ by locally filtering the measurement output signal $y_I(k)$

$$Y_I(k) \triangleq H(z)\left[y_I(k)\right] \tag{14}$$

and the output estimates as

$$\widehat{Y}_I(k) \triangleq H(z)\left[\tilde{x}_I(k)\right]. \tag{15}$$

[4]For example, consider the case shown in Fig. 1: subsystems Σ_1 and Σ_2 share the state variable $x^{(2)}$ while subsystems Σ_2 and Σ_3 share the state variable $x^{(4)}$. Thus, $x^{(2)} = x_1^{(2)} = x_2^{(1)}$ and $x^{(4)} = x_2^{(3)} = x_3^{(1)}$.

The residual constitutes the basis of the fault detection scheme. It can be compared, component by component, to a suitable adaptive detection threshold $\bar{r}_I \in \mathbb{R}^{n_I^x}$, thus generating a local fault decision attesting the status of the subsystem: healthy or faulty. A fault in the overall system is said to be detected when $|r_I^{(i)}(k)| > \bar{r}_I^{(i)}(k)$, for at least one component i in any Ith LFD.

We now analyze the filtered measurements and estimates

$$\begin{aligned} Y_I(k) &= H(z)\left[y_I(k)\right] = H(z)\left[x_I(k) + \xi_I(k)\right] \\ &= H_p(z)\left[z\left[x_I(k)\right]\right] + \Xi_I(k). \end{aligned} \tag{16}$$

In the absence of any faults (i.e., $\phi_I(x_I(k), z_I(k), u_I(k), k) = 0$), (16) becomes

$$\begin{aligned} Y_I(k) &= H_p(z)\left[x_I(k+1) + z\left[x_I(0)\delta(k)\right]\right] + \Xi_I(k) \\ &= H_p(z)\left[f_I\left(x_I(k), u_I(k)\right) + g_I\left(x_I(k), z_I(k), u_I(k)\right)\right] \\ &\quad + h(k)x_I(0) + \Xi_I(k) \end{aligned} \tag{17}$$

where $\delta(k)$ denotes the discrete-time unit-impulse sequence.

The filtered output estimation model for Y_I, denoted by $\widehat{Y}_I$, can be analyzed from the estimate provided by (12) as follows:

$$\begin{aligned} \widehat{Y}_I^{(s_I)}(k) = \sum_{J\in\mathcal{O}_s} W_s^{(I,J)} H_p(z) \Bigg[\Big(f_J^{(s_J)}\left(y_J(k), u_J(k)\right) \\ + \hat{g}_J^{(s_J)}\Big(y_J(k), v_J^b(k), u_J(k), \hat{\vartheta}_J(k)\Big)\Big)^b\Bigg] + h(k) y_I^{(s_I)}(0). \end{aligned} \tag{18}$$

Therefore, the residual (13) is readily computable from (14) and (15). The residual is analyzed in Section IV-D to obtain a suitable adaptive detection threshold. Now, we design the adaptive approximator $\hat{g}_I$, needed to compute the state estimate (12) and hence (15).

B. Adaptive Approximator

Reducing the uncertainty on the interconnection function enables improved detection thresholds which, in turn, results in better detection capabilities. In this subsection, we consider the design of a nonlinear adaptive approximator, exploiting the variables available in the local buffers in each LFD to manage communication delays (the details of the delay compensation strategy are given in Section IV-C). The structure of the linear-in-the-parameters nonlinear multivariable approximator is not dealt with in this paper (nonlinear approximation schemes like neural networks, fuzzy logic networks, wavelet networks, spline functions, polynomials, etc. can be used).

As shown later on in this subsection, adaptation of the parameters $\hat{\vartheta}_I$ of the approximator is achieved through the design of a dynamic state estimator which, in the general case of shared variables, takes on the form

$$\begin{aligned} &\hat{x}_I^{(s_I)}(k+1) \\ &= \lambda\Big(\hat{x}_I^{(s_I)}(k) - y_I^{(s_I)}(k)\Big) + \lambda \sum_{J\in\mathcal{O}_s} W_s^{(I,J)}\Big[\hat{x}_J^{b(s_J)}(k) - \hat{x}_I^{(s_I)}(k)\Big] \\ &\quad + \sum_{J\in\mathcal{O}_s} W_s^{(I,J)}\Big[f_J^{(s_J)}(y_J, u_J) + \hat{g}_J^{(s_J)}\Big(y_J, v_J^b, u_J, \hat{\vartheta}_J\Big)\Big]^b \end{aligned} \tag{19}$$

where $0 < \lambda < 1$ is a design parameter. Let us introduce the estimation error

$$\epsilon_I(k) \triangleq y_I(k) - \hat{x}_I(k)$$

and let us analyze ϵ_I under healthy mode of behavior. By assumption, $\sum_{J\in\mathcal{O}_s} W_s^{(I,J)} = 1$ and the following holds for shared variables, $\forall J \in \mathcal{O}_s$ (see the model decomposition procedure outlined in [5]):

$$\begin{aligned} &f^{(s)}(x,u) + \eta^{(s)}(x,u,k) \\ &\quad = f_J^{(s_J)}(x_J, u_J) + g_J^{(s_J)}(x_J, z_J, u_J) \\ &\quad = \sum_{J\in\mathcal{O}_s} W_s^{(I,J)}\left[f_J^{(s_J)}(x_J, u_J) + g_J^{(s_J)}(x_J, z_J, u_J)\right]. \end{aligned}$$

Moreover, we can write

$$\begin{aligned} &\sum_{J\in\mathcal{O}_s} W_s^{(I,J)}\left[f_J^{(s_J)}(x_J, u_J) + g_J^{(s_J)}(x_J, z_J, u_J)\right] \\ &\qquad = \sum_{J\in\mathcal{O}_s} W_s^{(I,J)}\left[f_J^{(s_J)}(x_J, u_J) + g_J^{(s_J)}(x_J, z_J, u_J)\right]^b \end{aligned}$$

thanks to the fact that only up-to-date information is used in the consensus mechanism by using the time-varying consensus matrix (see Section IV-C and E): in the case of delays, only the updated information is used.

Owing to these considerations, we compute the s_Ith state estimation error component, for the general form of (19), as follows:

$$\begin{aligned} &\epsilon_I^{(s_I)}(k+1) \\ &\quad = y_I^{(s_I)}(k+1) - \hat{x}_I^{(s_I)}(k+1) \\ &\quad = \sum_{J\in\mathcal{O}_s} W_s^{(I,J)}\left[\lambda\epsilon_J^{(s_J)} + \Delta f_J^{(s_J)} + \Delta g_J^{(s_J)} - \lambda\xi_J^{(s_J)}\right]^b \\ &\qquad + \lambda\xi_I^{(s_I)}(k) + \xi_I^{(s_I)}(k+1) \end{aligned} \tag{20}$$

where

$$\begin{aligned} \Delta f_J^{(s_J)} &\triangleq f_J^{(s_J)}(x_J, u_J) - f_J^{(s_J)}(y_J, u_J) \\ \Delta g_J^{(s_J)} &\triangleq g_J^{(s_J)}(x_J, z_J, u_J) - \hat{g}_J^{(s_J)}(y_J, v_J^b, u_J, \hat{\vartheta}_J). \end{aligned}$$

Let us introduce a compact formulation in vectorial form of the state error (20) for the sake of analysis. Specifically, we define for every sth state component the extended estimation error vector $\epsilon_{s,E}$, which is a column vector collecting the estimation error vectors of the N sub-systems sharing the sth state component: $\epsilon_{s,E} \triangleq \mathrm{col}(\epsilon_J^{(s_J)} : J \in \mathcal{O}_s)$. Notice that, if the sth state component is not shared, the set is just made of a single component. The dynamics of $\epsilon_{s,E}$ can be described as

$$\begin{aligned} \epsilon_{s,E}(k+1) = W_s\left[\lambda\epsilon_{s,E} + \Delta f_{s,E} + \Delta g_{s,E} - \lambda\xi_{s,E}\right]^b \\ + \lambda\xi_{s,E}(k) + \xi_{s,E}(k+1) \end{aligned} \tag{21}$$

where $\Delta f_{s,E}$ is a column vector, collecting the values $\Delta f_J^{(s_J)}$, for each $J \in \mathcal{O}_s$; $\Delta g_{s,E}(k)$ and $\xi_{s,E}$ are defined in an analogous way as $\Delta f_{s,E}(k)$. From this equation, the following learning law can be derived using Lyapunov stability methods (see [46]) for every $I \in 1, \ldots, N$:

$$\hat{\vartheta}_I(k+1) = P_{\hat{\Theta}_I}\Big[\hat{\vartheta}_I(k) + \gamma_I L_I^\top\left[\epsilon_I(k+1) - \lambda\epsilon_I(k)\right]\Big] \tag{22}$$

where $L_I^\top = \partial\hat{g}_I/\partial\hat{\vartheta}_I$ is the gradient matrix of the online approximator with respect to its adjustable parameters and

$\gamma_I = \mu_I/\varepsilon_I + \|L_I^\top\|_F^2$, with $P_{\hat{\Theta}_I}$ being a projection operator restricting $\hat{\vartheta}_I$ within $\hat{\Theta}_I$ [47], $\|\cdot\|_F$ denotes the Frobenius norm, and $\varepsilon_I > 0, 0 < \mu_I < 2$ are design constants that guarantee the stability of the learning law [47].

C. Delay Compensation Strategy

Next, we analyze the properties of the fault detection estimator introduced in (Section IV-A), where the filtered measurements are used; in particular, we explain how the estimator manages delays and packet losses in the second-level communication network between diagnosers.

In order to compute (12) and (19), the generic Jth diagnoser communicates to the neighboring LFDs the current values of the terms $\hat{x}_J^{(s_J)}$, $f_J^{(s_J)} + \hat{g}_J^{(s_J)}$ and v_I. It is worth noting that this information exchange between diagnosers can be affected by time-varying delays and packet losses, and hence a compensation strategy has to be devised.[5] It is important to note that a resynchronization strategy like the one used in the first-level communication networks cannot be used in this case, since here we consider data exchanged between different LFDs, and each LFD, of course, does not know the model of neighboring subsystems.

As in [43], thanks to the use of the virtual timestamps, the most recent measurements and information are considered. When a data packet arrives, its virtual timestamp v_{TS} is compared to t_b, which is the virtual timestamp of the information already in the buffer. If $v_{\mathrm{TS}} > t_b$, then the novel data packet takes its place in the buffer and $t_b \leftarrow v_{\mathrm{TS}}$. At time t_c, with $k < t_c < k+1$, each LFD computes the estimates for the time instant $k+1$ using information referred to time k. A variable in the buffer is up-to-date if $t_b = k$. Should a delay or a packet loss occur in the second-level communication network, we proceed as follows.

- If some of the interconnection variables are not up-to-date, that is $t_b < k$, then the learning of the interconnection function g_I (22) is temporarily paused. Anyway, not up-to-date interconnection variables are used to compute the local value of the interconnection function in the state estimators (12) and (19), but this error is taken into account in the computation of the detection threshold, as will be seen in the following subsection.
- The summations in (12) and (19) are carried on only using up-to-date terms.

In order to allow the implementation of this second strategy, we adopt a time-varying weighting matrix W_s, able to exclude from the summations in (12) and (19) the terms that are outdated (see Section IV-E).

D. Detection Threshold

In order to define an appropriate threshold for the detection of faults, we now analyze the dynamics of the output estimation error when the system is under healthy mode of behavior. Since, from (17) we have

$$Y_I^{(s_I)}(k) = \sum_{J\in\mathcal{O}_s} W_s^{(I,J)} \Big[H_p(z)\Big[f_J^{(s_J)}(x_J(k), u_J(k)) + g_J^{(s_J)}(x_J(k), z_J(k), u_J(k))\Big]\Big] + h(k)x_I^{(s_I)}(0) + \Xi_I^{(s_I)}(k) \tag{23}$$

we are able to compute the residual defined in (13) by using (18) and (23)

$$r_I^{(s_I)}(k) = \sum_{J\in\mathcal{O}_s} W_s^{(I,J)}\Big[\chi_J^{(s_J)}(k)\Big]^b - \xi_I^{(s_I)}(0)h(k) + \Xi_I^{(s_I)}(k) \tag{24}$$

where the total uncertainty term $\chi_J^{(s_J)}(k)$ is defined as

$$\chi_J^{(s_J)}(k) \triangleq H_p(z)\left[\Delta f_J^{(s_J)}(k) + \Delta g_J^{(s_J)}(k)\right]. \tag{25}$$

The interconnection function error Δg_I can be computed as the sum of four different terms

$$\Delta g_I = L_I\tilde{\vartheta}_I + \nu_I + \Delta\hat{g}_I + \Delta g_I^\tau. \tag{26}$$

The first term takes into account the error due to the parameters' estimation. This error can be characterized by introducing an *optimal weight vector* [48] $\hat{\vartheta}_I^*$ as follows:

$$\hat{\vartheta}_I^* \triangleq \arg\min_{\hat{\vartheta}_I} \sup_{x_I, z_I, u_I} \left\| g_I(x_I, z_I, u_I) - \hat{g}_I(x_I, z_I, u_I, \hat{\vartheta}_I \right\| \tag{27}$$

with $\hat{\vartheta}_I, x_I, z_I, u_I$ taking values in their respective domains, and by defining the parameter estimation error

$$\tilde{\vartheta}_I \triangleq \hat{\vartheta}_I^* - \hat{\vartheta}_I.$$

The second term in (26) is the so-called *minimum functional approximation error* ν_I, which describes the least possible approximation error that can be obtained at time k if $\hat{\vartheta}_I$ were optimally chosen

$$\nu_I(k) \triangleq g_I(x_I, z_I, u_I) - \hat{g}_I\left(x_I, z_I, u_I, \hat{\vartheta}_I^*\right).$$

Then, a term representing the error caused by the use of the uncertain measurements instead of the actual values of the state variables is defined

$$\Delta\hat{g}_I \triangleq \hat{g}_I(x_I, z_I, u_I, \hat{\vartheta}_I) - \hat{g}_I(y_I, v_I, u_I, \hat{\vartheta}_I).$$

Finally, the estimation error due to the use of delayed measurements is taken into account by

$$\Delta g_I^\tau \triangleq \hat{g}_I(y_I, v_I, u_I, \hat{\vartheta}_I) - \hat{g}_I\left(y_I, v_I^b, u_I, \hat{\vartheta}_I\right)$$

where v_I is the current measured variable and v_I^b is the value in the buffer, which is "old" in the presence of delays. Clearly, $\Delta g_I^\tau = 0$ when up-to-date measurements are used (in this case, $v_I^b = v_I$).

[5] The delay compensation strategy is derived without any assumption on the delay length, thus eventually dealing with the problem of packet losses and "out-of-sequence" packets. We assume that the communication network between diagnosers is designed so to avoid pathological scenarios, such as, for example, a situation in which the communication delay is always larger than the sampling time.

Using (26), the total uncertainty term $\chi_J^{(s_J)}(k)$ in (25) can be rewritten as

$$\chi_J^{(s_J)}(k) \triangleq H_p(z)\Big[\Delta f_J^{(s_J)}(k) + L_J^{(s_J)}\tilde{\vartheta}_J(k) + \nu_J^{(s_J)}(k) + \Delta\hat{g}_J^{(s_J)}(k) + \Delta g_J^{\tau^{(s_J)}}(k)\Big] \quad (28)$$

where $L_J^{(s_J)}$ indicates the s_Jth line of the matrix L_J. Using the triangle inequality, (24) satisfies

$$\begin{aligned}\left|r_I^{(s_I)}(k)\right| &\leq \left|\sum_{J\in\mathcal{O}_s} W_s^{(I,J)}\left[\chi_J^{(s_J)}(k)\right]^b\right| + \left|\xi_I^{(s_I)}(0)h(k)\right| + \left|\Xi_I^{(s_I)}(k)\right| \\ &\leq \sum_{J\in\mathcal{O}_s} W_s^{(I,J)}\left[\left|\chi_J^{(s_J)}(k)\right|\right]^b + \bar{\xi}_I^{(s_I)}(0)|h(k)| + \bar{\Xi}_I^{(s_I)}(k).\end{aligned} \quad (29)$$

From (28) and using again the triangle inequality, we obtain

$$\begin{aligned}\left|\chi_J^{(s_J)}(k)\right| &\leq \left|H_p(z)\left[\Delta f_J^{(s_J)}(k) + \Delta g_J^{(s_J)}(k)\right]\right| \\ &\leq \sum_{n=0}^{k}|h_p(k-n)|\Big|\Delta f_J^{(s_J)}(n) + L_J^{(s_J)}\tilde{\vartheta}_J(n) + \nu_J^{(s_J)}(n) \\ &\qquad + \Delta\hat{g}_J^{(s_J)}(n) + \Delta g_J^{\tau^{(s_J)}}(n)\Big| \\ &\leq \bar{\chi}_J^{(s_J)}(k) \triangleq \bar{H}_p(z)\left[\bar{\Delta} f_J^{(s_J)}(k) + \bar{\Delta} g_J^{(s_J)}(k)\right]\end{aligned} \quad (30)$$

where $\bar{H}_p(z)$ is the transfer function with impulse response $\bar{h}_p(k) = |h_p(k)|$

$$\begin{aligned}\bar{\Delta} f_J^{(s_J)}(k) &\triangleq \max_{\left|\xi_J^{(s_J)}\right|\leq\bar{\xi}_J^{(s_J)}}\left\{\left|\Delta f_J^{(s_J)}(k)\right|\right\} \\ \bar{\Delta} g_I^{(s_J)}(k) &\triangleq \left\|L_I^{(s_J)}\right\|\kappa_I(\hat{\vartheta}_I) + \bar{\nu}_I^{(s_J)}(k) \\ &\quad + \max_{|\xi_I|\leq\bar{\xi}_I(k)}\max_{|\varsigma_I|\leq\bar{\varsigma}_I(k)}\left|\Delta\hat{g}_I^{(s_J)}(k)\right| \\ &\quad + \max_{v_I\in\mathcal{R}^v}\Big|\hat{g}_I^{(s_J)}(y_I, v_I, u_I, \hat{\vartheta}_I) \\ &\qquad - \hat{g}_I^{(s_J)}\left(y_I, v_I^b(t_b), u_I, \hat{\vartheta}_I\right)\Big|\end{aligned} \quad (31)$$

with $\bar{\nu}_I$ denoting a bound to the minimum functional approximation error, the function κ_I being such that $\kappa_I(\hat{\vartheta}_I) \geq \|\tilde{\vartheta}_I\|$ and $\mathcal{R}^{v_I} \subset \mathbb{R}^{q_I}$, where this last term represents a local domain of the interconnection variable and is communicated by the neighboring LFDs at $k = 0$. It is important to remark that $\mathcal{R}^{v_I}$ coincides with the domain $\mathcal{R}^{x_J}$ for subsystem J (Assumption 1). Thanks to the way the threshold is designed from (29), it is straightforward that it guarantees the absence of false alarms, since the residual *prior to the fault occurrence* always satisfies

$$\left|r_I^{(s_I)}(k)\right| \leq \bar{r}_I^{(s_I)}(k)$$

where the detection threshold $\bar{r}_I^{(s_I)}$ is defined as

$$\bar{r}_I^{(s_I)}(k) \triangleq \sum_{J\in\mathcal{O}_s} W_s^{(I,J)}\left[\bar{\chi}_J^{(s_J)}(k)\right]^b + \bar{\xi}_I^{(s_I)}(0)\,|h(k)| + \bar{\Xi}_I^{(s_I)}(k). \quad (32)$$

The threshold term $\bar{\chi}_J^{(s_J)}$ is computed at node J, collected in the information vector $I_{J,I}$, and sent to neighboring LFD I.

Remark 4: Notice that, even in the case of a conservative bound $\bar{\xi}_I^{(s_I)}$, the second term $\bar{\xi}_I^{(s_I)}|h(k)|$ affects the detection threshold only during the initial portion of the transient (the impulse response $h(k)$ of the filter $H(z)$ decays exponentially). Moreover, the term $\bar{\Xi}_I^{(s_I)}$ in (31) takes into account the uncertainty due to the delays in the communication network between LFDs. This term is instrumental to ensure the absence of false alarms caused by these communication delays.

Remark 5: The terms $\bar{\xi}_I(k)$ and $\bar{\varsigma}_I(k)$ are computed by the LFDs at each time step after the resynchronization task [see (8)] and are available to compute the fault detection threshold.

Remark 6: Admittedly, the bounds used in (30) and (31) give rise to conservative thresholds but have the advantage of guaranteeing the absence of false-positive alarms and of being easily computable requiring a small amount of data to be exchanged between the LFDs. In the presence of *a priori* knowledge on the process to be monitored, a tighter bound could be devised (for example, Lipschitz conditions on the local models could be easily exploited to devise tighter detection thresholds.

E. Time-Varying Consensus Mechanism

In this subsection, the consensus methodology concerning shared state variables is modified in order to address the conservativeness of the detection threshold (32). More specifically, the consensus-weighting matrix W_s takes on the following time-varying form:

$$W_s^{(I,J)} = \begin{cases} 1 & \text{if } J = \arg\min_{J\in\mathcal{O}_s^b}\left[\bar{\chi}_J^{(s_J)}(k)\right]^b \\ 0 & \text{otherwise}\end{cases} \quad (33)$$

where $\mathcal{O}_s^b$ is the time-varying set of subsystems sharing s at time k for which the Ith LFD has up-to-date information in the buffer. In intuitive terms, the time behavior (33) ensures that a larger weight is assigned to the subsystem characterized by the lowest threshold (hence, in rough terms, lowest uncertainty in its measurements and in the local model and with the smallest level of delays and packet losses).

It is important to remark that the consensus protocol uses only up-to-date information. This means that at each step each LFD uses only the information received from one LFD sharing the considered variable, and this choice can change at each step. It is possible that neighboring LFDs sharing the same variable $x^{(s)}$ use different information for their threshold, since the threshold term $\bar{\chi}_J^{(s)}(k)$ depends on the reliability of the communication links, in conjunction with the confidence that each LFD has in its own measurements and estimates. In this way, moreover, we can manage time delays and packet losses: in fact, if the FDAE does not receive some consensus terms from some neighboring LFDs, it simply considers and weights only the up-to-date values. It is worth noting that this approach can be used in any case, with or without delays, and in Section V we demonstrate that it improves detectability.

In the following simple results, the boundedness of the estimation error is addressed when the time-varying consensus matrix (33) is used.

Proposition 4.1: The error dynamics (21), where the consensus matrix is updated according to (33), is BIBO stable.

Proof: Since W_s is a stochastic matrix, its norm is identically equal to 1. Therefore, since $0<\lambda<1$, $\|\lambda W_s(k)\|\leq\gamma<1$, with $0<\gamma<1$. Let us define

$$U_{s,E}(k)=W_s[\Delta f_{s,E}+\Delta g_{s,E}-\lambda\xi_{s,E}]^b+\lambda\xi_{s,E}(k)+\xi_{s,E}(k+1). \tag{34}$$

We have

$$\begin{aligned}
&\|\epsilon_{s,E}(k+1)\| \\
&\quad\leq \|\lambda W^s(k)\epsilon_{s,E}(k)\|+\|U_{s,E}(k)\| \\
&\quad\leq \|\lambda W^s(k)\|\,\|\lambda W^s(k-1)\|\ldots\|\lambda W^s(0)\|\,\|\epsilon_{s,E}(0)\| \\
&\qquad+\sum_{j=1}^{k}\|\lambda W^s(k)\|\|\lambda W^s(k-1)\|\ldots\|\lambda W^s(j)\|\,\|U_{s,E}(j)\| \\
&\quad\leq \gamma^k\,\|\epsilon_{s,E}(0)\|+\sum_{j=1}^{k}\gamma^{k-j}\,\|U_{s,E}(j)\| \\
&\quad\leq \frac{1}{1-\gamma}\sup_{j\geq1}\|U_{s,E}(j)\|\,.
\end{aligned}$$

For $k\to\infty$, the unforced system converges to zero and the series converges to a bounded value (see results in [49]). Moreover, using results in [50] for unforced systems, we can state that a system $x(k+1)=A(k)x(k)$, with $A(k)\in\text{conv}(A_1,\ldots,A_N)$, is exponentially stable if and only if $\exists$ a sufficiently large integer q such that $\|A_{i_1}A_{i_2},\ldots,A_{i_q}\|\leq\gamma<1,\ \forall(i_1,\ldots,i_q)\in\{1,\ldots,N\}^q$. In our case, therefore, we only need to analyze matrix $W^s(k)$. Since each row of $W^s(k)$ has all null elements except one equal to 1, the product $W^s(k)W^s(k-1),\ldots,W^s(0)$ is a stochastic matrix. Hence, since $0<\lambda<1$, we have $\|\lambda^t(W^s(k)W^s(k-1),\ldots,W^s(0))\|<1$ and the hypothesis is satisfied. Finally, since all the uncertain terms are bounded, then the discrete-time system (21) is BIBO stable. ■

F. Local Fault Detection Algorithm

Now, all the elements needed to implement the proposed fault detection scheme are available. For the sake of clarity, the implementation of the local fault detection methodology is sketched in Algorithm 1.

Algorithm 1 Fault detection algorithm for the Ith LFD

```
Learning = ON
Initialize the estimate x̂_I(0) = y_I(0)
Initialize the estimate x̃_I(0) = y_I(0)
Compute the estimate x̂_I(1) (19)
Compute the estimate x̃_I(1) (12)
Set k = 1
while A fault is not detected do
   Measurements y_I(k) are acquired
   Compute ε_I(k) = y_I(k) − x̂_I(k) (for learning)
   Compute Y_I(k) (14), Ŷ_I(k) (15)
   Compute the residual r_I(k) = Y_I(k) − Ŷ_I(k)
   Information from neighbors is acquired
   Update consensus weights (33)
   Compute the threshold r̄_I(k) (32)
   Compare |r_I(k)| with r̄_I(k)
   if |r_I(k)| > r̄_I(k) then
      A fault is detected
      Learning = OFF
   end if
   if Some components i of v_I(k) are not received then
      Learning = OFF
   else
      Learning = ON
      v_I^{b(i)}(k) = v_I^{(i)}(k)
   end if
   if Learning = ON then
      Update ϑ̂_I(k) (22)
   else
      ϑ̂_I(k) = ϑ̂_I(k − 1)
   end if
   Compute the novel estimate x̂_I(k + 1) (19)
   Compute the novel estimate x̃_I(k + 1) (12)
   k = k + 1
end while
```

V. Detectability Conditions

In this section, we address some sufficient conditions for detectability of faults by the proposed distributed networked fault detection scheme, thus considering the behavior of the fault detection algorithm in the case of a faulty system. We assume that at an unknown time k_0 a fault ϕ occurs. Let us consider the general case of a variable shared among more than one subsystem. The fault detectability analysis constitutes a theoretical result that characterizes quantitatively (and implicitly) the class of faults detectable by the proposed scheme.

Theorem 5.1 (Fault Detectability): A fault in the Ith subsystem occurring at time $k=k_0$ is detectable at a certain time $k=k_d$ if the fault function $\phi_I^{(s_I)}(x_I,z_I,u_I,k_d)$ satisfies the following inequality for some $s_I=1,\ldots,n_I^x$:

$$\left|\sum_{n=k_0}^{k_d}h_p(k-n)\phi_I^{(s_I)}(x_I,z_I,u_I,n)\right|>2\bar{r}_I^{(s_I)}(k_d). \tag{35}$$

Proof: After fault occurrence, that is, for $k>k_0$, (24) becomes

$$\begin{aligned}
&r_I^{(s_I)}(k) \\
&\quad=\sum_{J\in\mathcal{O}_s}W_s^{(I,J)}\left[\chi_J^{(s_J)}(k)^b+H_p(z)\left[\phi_J^{(s_J)}(x_J,z_J,u_J,k)\right]\right] \\
&\qquad-\xi_I^{(s_I)}(0)h(k)+\Xi_I^{(s_I)}(k) \\
&\quad=\sum_{J\in\mathcal{O}_s}W_s^{(I,J)}\left[\chi_J^{(s_J)}(k)\right]^b-\xi_I^{(s_I)}(0)h(k)+\Xi_I^{(s_I)}(k) \\
&\qquad+H_p(z)\left[\phi_I^{(s_I)}(x_I,z_I,u_I,k)\right]. \qquad (36)
\end{aligned}$$

Using the triangle inequality, from (36) we can write

$$\begin{aligned}
\left|r_I^{(s_I)}(k)\right|\geq&-\left|\sum_{J\in\mathcal{O}_s}W_s^{(I,J)}\left[\chi_J^{(s_J)}(k)\right]^b\right|-\left|\xi_I^{(s_I)}(0)h(k)\right| \\
&-\left|\Xi_I^{(s_I)}(k)\right|+\left|H_p(z)\left[\phi_I^{(s_I)}(x_I,z_I,u_I,k)\right]\right| \qquad (37)
\end{aligned}$$

and by using a similar procedure as in the derivation of (32) and (37) becomes

$$\left|r_I^{(s_I)}(k)\right| \geq -\bar{r}_I^{(s_I)}(k) + \left|H_p(z)\left[\phi_I^{(s_I)}(x_I, z_I, u_I, k)\right]\right|. \tag{38}$$

For fault detection at time $k = k_d$, the inequality $|r_I^{(s_I)}(k_d)| > \bar{r}_I^{(s_I)}(k_d)$ must hold for some $i = 1, \ldots, n_I^x$, so the final fault detectability condition is obtained

$$\left|H_p(z)\left[\phi_I^{(s_I)}(x_I, z_I, u_I, k_d)\right]\right| > 2\bar{r}_I^{(s_I)}(k_d).$$

This can be rewritten in the summation form (35) of the theorem. ■

This theorem provides a sufficient condition for the implicit characterization of a class of faults that can be detected by the proposed fault detection scheme. Based on this result, in (35) it is easy to see that the lower the threshold is, the sooner the fault will be detected. Therefore the use of filtering along with the proposed time-varying consensus weighting matrix, able to choose the lowest threshold components in the case of shared variables, improves detectability. It is worth noting that this is true in general, also in the case without delays. Besides, let us note that the detectability condition represents the minimum cumulative magnitude of the fault that can be detected under a specific trajectory of the system. It is possible to study offline this condition for representative trajectories of the system.

Remark 7: The use of filtering is of crucial importance in order to derive tight detection thresholds that guarantee no false alarms. As it can be seen in the detectability condition given in (35), the detection of the fault depends on the filtered fault function ϕ_I. As a result, the selection of the filter plays a crucial role to the proposed scheme. A rigorous investigation of the filtering impact (according to the poles' location and filters' order) on the detection time under continuous time is presented in [42].

VI. Simulation Results

In this section, we present some simulation results in order to illustrate the effectiveness of the proposed methods.

A. Simulation System

We consider a five-tank system [51], monitored by two LFDs (see Fig. 4). The two LFDs monitor three tanks each and share the third tank. The local nominal functions f_1 and f_2 describe the flows through the pipes linking tanks assigned to the same LFD, while the interconnection terms g_1 and g_2 are due to the flow between tanks 3 and 4 and between tanks 2 and 3, respectively. The monolithic system (see Fig. 4) is decomposed into two overlapping subsystems. By using the formalism presented in [5], the decomposition is $\mathcal{D} = \{\Sigma_1, \Sigma_2\}$, with index sets $\mathcal{I}_1 = [1\ 2\ 3]^\top$ and $\mathcal{I}_2 = [3\ 4\ 5]^\top$, representing the state variables indices belonging to each subsystem. The third tank is shared, and therefore the corresponding overlap index set is $\mathcal{O}_3 = \{1, 2\}$. The tank levels are denoted by $x_I^{(i)}$, with $I = \{1, 2\}$ and $i = \{1, 2, 3\}$, and are limited between 0 and 10 m. Two pumps are present, feeding the first and the fifth tank with the following flows: $u_1 = 1.25 + 0.25 \cdot \sin(0.25 \cdot k)$ and $u_2 = 1.75 + 0.4 \cdot \cos(0.05 \cdot k)$. The nominal tank sections

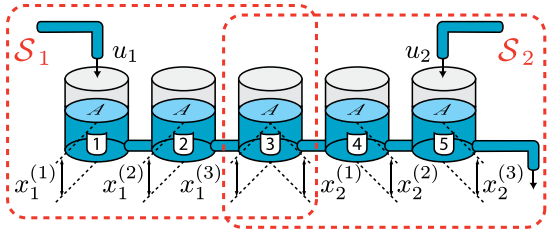

Fig. 4. Structure of the five-tank system.

are $A = [1\ 1\ 1\ 1\ 1]$ m^2, while the interconnecting pipe cross-sections are nominally equal to $A_p = [0.1\ 0.1\ 0.1\ 0.1\ 0.1]$ m^2. For each tank, there are connected drain pipes whose nominal cross-section are $A_d = [0.05\ 0.05\ 0.05\ 0.05\ 0.05]$ m^2. All the pipes outflow coefficients are unitary. By using balance equations and Torricelli's rule, we obtain the state equations (for details about the dynamical equations of a multitank system see as example [46]). The actual cross-sections used are affected by random uncertainties no larger than 7.5% and 10% of the nominal values, respectively for the tanks and for the pipes. The tank initial levels and the outflow coefficients are affected by uncertainties no larger than 15%. Furthermore the tank levels measurements m_I are affected by measurement noise w_I whose components are upper bounded by $\bar{w}_1 = [0.05\ 0.05\ 0.05]$ m and $\bar{w}_2 = [0.05\ 0.05\ 0.05]$ m. The virtual measurement errors are computed online basing on the resynchronization process. In order to learn the interconnection functions of each subsystem, which consist on the flows through pipes crossing a subsystem boundary, each LFD is provided with adaptive approximators $\hat{g}_I$, implemented by RBF neural networks having 3 and 2 neurons respectively along the range of each input dimension. Since the interconnection variables are $z_1 = x_2^{(2)}$ and $z_2 = x_1^{(2)}$, the interconnection functions $g_1(x_1, z_1, u_1)$ and $g_2(x_2, z_2, u_2)$ should be 5-input, 3-output functions. On the other hand, because of the topology of the specific system, both g_1 and g_2 have only one nonzero output component and depend only on $(x_2^{(2)}, x_1^{(3)})$ and $(x_1^{(2)}, x_2^{(1)})$ respectively. Therefore, the adaptive approximators $\hat{g}_1$ and $\hat{g}_2$ were realized with two 2-input, 1-output radial basis neural networks. The networks to learn $\hat{g}_1$ and $\hat{g}_2$ are implemented with nine basis functions. After suitable offline simulations, the parameter domains Θ_I were chosen to be hyperspheres with radii equal to $[4\ 4] \cdot T_s$, with $T_s = 0.1$ s being the sampling period. The learning rate auxiliary coefficients for the interconnection adaptive approximators were set to $\mu_{1,0} = 0.005$, $\varepsilon_{1,0} = 10^{-3}$, $\mu_{2,0} = 0.005$, $\varepsilon_{2,0} = 10^{-3}$, while the learning filter constants were all set to $\lambda = 0.85$. On the other hand, the detection filter is designed having transfer function $(1 - \lambda)/(1 - \lambda z^{-1})$. The different sensor networks, each one measuring a single variable, have different sampling rates. The measurement sampling periods are [10 15 0.5 0.35 0.21 0.45 0.7], where the first two variables are the inputs, while the offsets with respect to the diagnosers clock are [0 0 0.1 0.25 0.13 0.15 0.07]. The measurements signals are shown in Fig. 5, where the real signals, the sampled measurements, and the projected signals are illustrated.

It is worth noting that the considered case includes a scenario in which also the input signals are subject to noise and sampling issues. The communication delays between diagnosers are

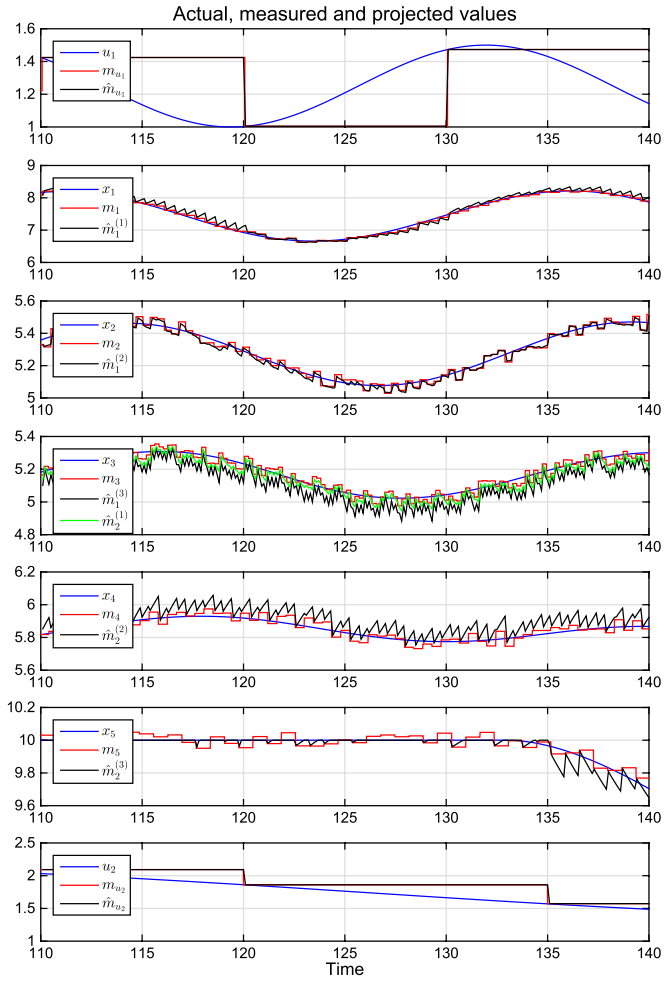

Fig. 5. Measured and projected signals.

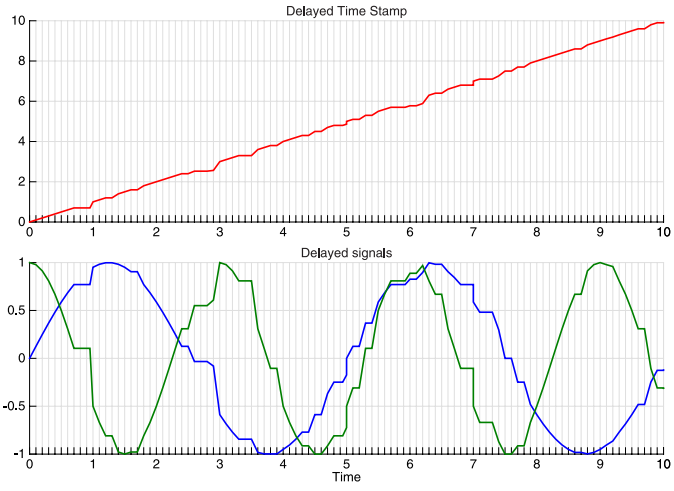

Fig. 6. Effect of the time-varying communication delays on transmitted signals and timestamps.

TABLE I
DETECTION ANALYSIS FOR SCENARIO NUMBER 1

case	T_d, LFD 1	T_d, LFD 2	MPORT, LFD 1	MPORT, LFD 2
ideal	200.8	201.0	1.798	1.44
real	200.5	201.2	1.346	1.200

random and time-varying: the effects of the delay are shown in Fig. 6 for the case of two sinusoidal signals as example. In the first plot, the received timestamp is illustrated, while the second figure shows the sinusoidal signals as they are received by the other diagnosers.

B. Simulation Scenarios and Results

We present three different simulation scenarios. In the first scenario, the considered fault function represents a leakage (a circular hole with cross section equal to 0.15 times the nominal tank section) in the third tank occurring at time $k = 200$ s. The simulation results are shown in Fig. 7, where the detection residuals and the time-varying thresholds are represented. It is possible to see that both the first and the second local fault diagnosers are able to detect the fault occurring on the third tank.

In particular, the fault is detected at time $k = 200.5$ s by LFD 1 and at $k = 201.2$ s by the second diagnoser. We compared the obtained results to the case in which all the measurements are synchronized and no communication delays are present, which is an ideal case. The model and fault parameters are the same used in the case with multirate measurements and delayed communication. As it is possible to see in Table I, in this ideal scenario, the first local fault diagnoser can detect the fault at time $k = 200.8$ s, while the detection time of the second LFD is $k = 201.0$. In Table I, another performance index is reported, that is, the *Maximum POst-detection Residual to Threshold* (MPORT) ratio. The reason for computing the MPORT ratio is that it gives a quantitative indication on how much the thresholds could increase, for instance for coping with larger uncertainty sources, continuing to detect anyway the fault. It could be defined, in other words, as an indicator of the robustness of the threshold with respect to the uncertainties sources. If it is high, the threshold should be able to detect the fault even in presence of a larger uncertainty.

In this example, simulation results show that the introduction of the resynchronization scheme and of the delay compensation strategy allows to obtain fault detection even when the measurements are nonsynchronized and the communication network is not reliable. Moreover, the detection time is comparable to the ideal case without delays.

In the second scenario, we consider the same system and the same kind of fault, thus a leakage, but with varying hole radii. The radii are chosen in order to correspond to hole sections between 0.15 and 0.5 times the tank nominal section. The differences with previous scenario are: the sampling time has been lowered to 0.025 s in order to better appreciate the effect of the fault magnitude on the detection time; the fault time has been set equal to $T_f = 15.1$ s and the fault time evolution is incipient instead of abrupt, with a time profile described by $\beta(k - k_0) = 1 - b^{-(k-k_0)}$, with $b = 250$ (see [5] for a definition of fault time profile). It is possible to see in Fig. 8, how the detection time and the MPORT ratios change depending on the different magnitude of the fault. This figure has been generated by averaging the results of 30 simulations run for each hole radius, with different random delays, packet losses, and model uncertainties. The two LFDs are not always able to both detect the fault, as for low values of the hole radius the fault is hidden by the uncertainties due to measurement asynchronicity, delays, and noise. In particular, the fault magnitude influences the

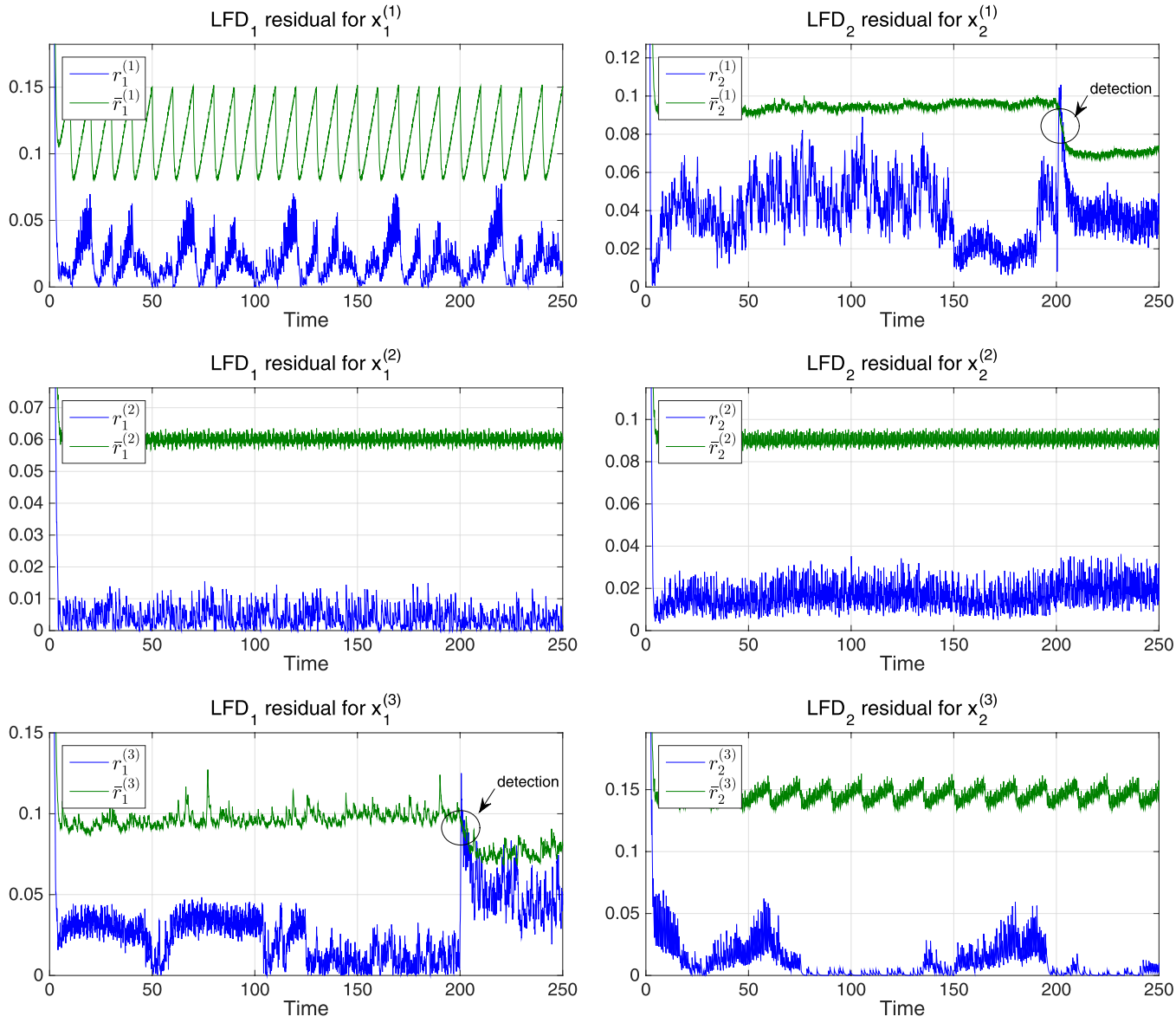

Fig. 7. Scenario no. 1: detection residuals and thresholds. The saw-tooth like behavior of the thresholds $\bar{r}_1^{(1)}$ and $\bar{r}_2^{(3)}$ is the effect of the virtual measurement error bound growing between one actual measurement of the pump inflows and the following one. As they are quite scarce, happening only every 10 and 15 s, this effect is noticeable.

detectability, with the detection time decreasing for larger fault magnitudes. Instead, the MPORT ratio shows a clear and almost linear, in this example, dependence on the fault magnitude. The results obtained considering this scenario show thus the importance of the detectability analysis. The magnitude of the fault is related to the possibility to detect the fault and to the robustness of the detection.

Finally, in the third scenario, we consider the same five-tank system and parameters as in the first scenario, but a different fault, that is, an actuator fault. At time $k = 150$ s, a fault on pump number 2 occurs, causing a reduction of the 35% of the flow. We assume that the fault function has again an incipient time profile $\beta(k - k_0) = 1 - b^{-(k-k_0)}$, with $b = 100$. Its development is thus quite smooth, and only tank 5 is affected by the fault. We can see the results in Fig. 9 for the component affected by the fault in LFD 2. For all the other components, the residuals are lower than the corresponding thresholds. Also in this scenario, the proposed fault detection architecture is able to detect the fault even in the worst conditions (delayed and asynchronous measurements). Due to the smoothness of the fault time profile, with respect to the leakage case, now the difference in the detection time between real and ideal conditions is larger. In the ideal case, we detect the fault at $k = 186.8$ s, 36 s after fault occurrence, with MPORT $= 1.21$, while in the real case we have detection at 191.7 s, 41 s after fault time, with MPORT $= 1.16$.

VII. Concluding Remarks

In this paper, a comprehensive architecture for the distributed fault diagnosis of large-scale nonlinear uncertain systems in a networked context has been presented. The proposed approach considers all the parts of the networked system: the physical environment, the sensor level, the local diagnosers layer, and the communication networks. The general distributed diagnosis approach presented in [5] is generalized in order

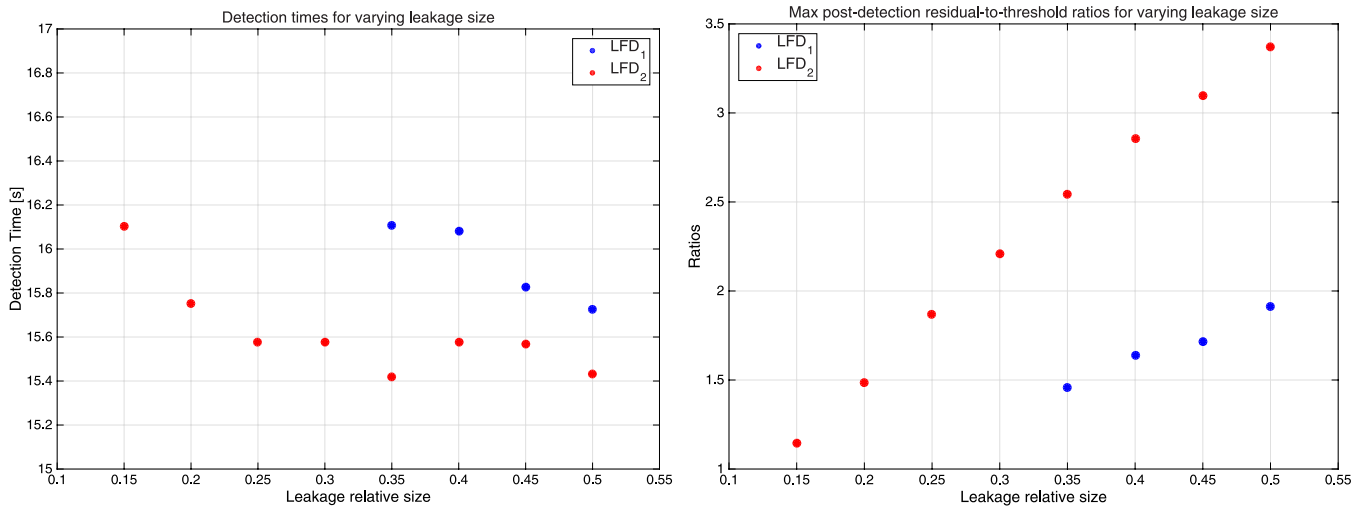

Fig. 8. Scenario no. 2: detection time and MPORT ratio versus leakage holes sections.

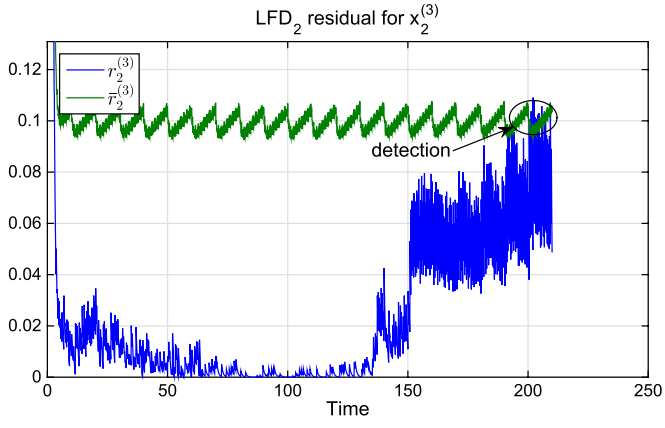

Fig. 9. Scenario no. 3: detection residuals and thresholds.

to address some of the issues emerging when designing distributed networked monitoring architectures. More specifically, multirate variable sampling systems have been considered and a model-based resynchronization mechanism has been proposed to be implemented by each local fault-diagnosis unit. Moreover, a delay compensation strategy is derived to face the problem of delays and packet dropouts in the communication networks. Finally, a general class of filters has been embedded into the design of the residual and threshold signals in order to filter measurement noise and derive less conservative detection thresholds.

As a future work, we will investigate the multiple faults case and the sensors faults scenario (see for example [52]–[54]).

References

[1] J. Baillieul and P. Antsaklis, "Control and communication challenges in networked real-time systems," *Proc. IEEE*, vol. 95, no. 1, pp. 9–28, Jan. 2007.

[2] E. Garcia, P. J. Antsaklis, and L. A. Montestruque, *Model-Based Control of Networked Systems*. New York, NY, USA: Springer, 2014.

[3] R. Patton, C. Kambhampati, A. Casavola, P. Zhang, S. Ding, and D. Sauter, "A generic strategy for fault-tolerance in control systems distributed over a network," *Eur. J. Control*, vol. 13, no. 2–3, pp. 280–296, 2007.

[4] F. Boem, R. M. G. Ferrari, and T. Parisini, "Distributed fault detection and isolation of continuous-time nonlinear systems," *Eur. J. Control*, no. 5/6, pp. 603–620, 2011.

[5] R. Ferrari, T. Parisini, and M. Polycarpou, "Distributed fault detection and isolation of large-scale discrete-time nonlinear systems: An adaptive approximation approach," *IEEE Trans. Autom. Control*, vol. 57, no. 2, pp. 275–290, Feb. 2012.

[6] F. Boem, R. M. Ferrari, T. Parisini, and M. M. Polycarpou, "Distributed fault diagnosis for continuous-time nonlinear systems: The input-output case," *Annu. Rev. Control*, vol. 37, no. 1, pp. 163–169, 2013.

[7] X. Zhang and Q. Zhang, "Distributed fault diagnosis in a class of interconnected nonlinear uncertain systems," *Int. J. Control*, vol. 85, no. 11, pp. 1644–1662, 2012.

[8] Q. Zhang and X. Zhang, "A distributed detection scheme for process faults and sensor faults in a class of interconnected nonlinear uncertain systems," in *Proc. 2012 IEEE 51st Conf. Decision Control*, 2012, pp. 586–591.

[9] C. Keliris and M. M. Polycarpou, "A distributed fault detection filtering approach for a class of interconnected continuous-time nonlinear systems," in *Proc. 2011 IEEE Conf. Decision Control Eur. Control Conf.*, 2011, pp. 89–94.

[10] V. Reppa, M. Polycarpou, and C. Panayiotou, "A distributed architecture for sensor fault detection and isolation using adaptive approximation," in *Proc. 2012 Int. Joint Conf. Neural Netw.*, 2012, pp. 1–8.

[11] X. Ge, Q.-L. Han, and X. Jiang, "Distributed fault detection for sensor networks with markovian sensing topology," in *Proc. Amer. Control Conf.*, 2013, pp. 3555–3560.

[12] N. S. Nokhodberiz and J. Poshtan, "Belief consensus-based distributed particle filters for fault diagnosis of non-linear distributed systems," in *Proc. Inst. Mechanical Engineers, Part I: J. Syst. Control Eng.*, 2013, Art. no. 0959651813512478.

[13] F. Boem, Y. Xu, C. Fischione, and T. Parisini, "Distributed fault detection using sensor networks and pareto estimation," in *Proc. 2013 Eur. Control Conf.*, 2013, pp. 932–937.

[14] E. Noursadeghi and I. Raptis, "Distributed fault detection of nonlinear large-scale dynamic systems," in *Proc. ACM/IEEE 6th Int. Conf. Cyber-Physical Systems*, ser. ICCPS'15. New York, USA: ACM, 2015, pp. 51–59. [Online]. Available: http://doi.acm.org/10.1145/2735960.2735981

[15] A. A. Cardenas, S. Amin, Z.-S. Lin, Y.-L. Huang, C.-Y. Huang, and S. Sastry, "Attacks against process control systems: Risk assessment, detection, and response," in *Proc. 6th ACM Symp. Information, Computer and Communications Security*, ser. ASIACCS'11. New York, USA: ACM, 2011, pp. 355–366.

[16] F. Dörfler, F. Pasqualetti, and F. Bullo, "Distributed detection of cyber-physical attacks in power networks: A waveform relaxation approach," in *Proc. 49th Annu. Allerton Conf. Commun. Control, Comp.*, 2011, pp. 1486–1491.

[17] F. Pasqualetti, F. Dörfler, and F. Bullo, "Attack detection and identification in cyber-physical systems—Part I: Models and fundamental limitations," Feb. 2012, unpublished manuscript. [Online]. Available: http://arxiv.org/abs/1202.6144

[18] F. Pasqualetti, F. Dörfler, and F. Bullo, "Attack detection and identification in cyber-physical systems—Part II: Centralized and distributed monitor design," Feb. 2012, unpublished manuscript. [Online]. Available: http://arxiv.org/abs/1202.6049

[19] F. Pasqualetti, F. Dörfler, and F. Bullo, "Cyber-physical attacks in power networks: Models, fundamental limitations and monitor design," in *Proc. 2011 IEEE Conf. Decision Control Eur. Control Conf.*, 2011, pp. 2195–2201.
[20] A. Teixeira, H. Sandberg, and K. Johansson, "Networked control systems under cyber attacks with applications to power networks," in *Proc. Amer. Control Conf.*, 2010, pp. 3690–3696.
[21] I. Shames, A. M. Teixeira, H. Sandberg, and K. H. Johansson, "Distributed fault detection for interconnected second-order systems," *Automatica*, vol. 47, no. 12, pp. 2757–2764, 2011.
[22] K. Zhang, B. Jiang, and V. Cocquempot, "Adaptive technique-based distributed fault estimation observer design for multi-agent systems with directed graphs," *IET Control Theory Appl.*, vol. 9, no. 18, pp. 2619–2625, 2015.
[23] M. Davoodi, K. Khorasani, H. Talebi, and H. Momeni, "Distributed fault detection and isolation filter design for a network of heterogeneous multiagent systems," *IEEE Trans. Control Syst. Technol.*, vol. 22, no. 3, pp. 1061–1069, May 2014.
[24] F. Arrichiello, A. Marino, and F. Pierri, "Observer-based decentralized fault detection and isolation strategy for networked multirobot systems," *IEEE Trans. Control Syst. Technol.*, vol. 23, no. 4, pp. 1465–1476, Jul. 2015.
[25] G. Pin and T. Parisini, "Networked predictive control of uncertain constrained nonlinear systems: Recursive feasibility and input-to-state stability analysis," *IEEE Trans. Autom. Control*, vol. 56, no. 1, pp. 72–87, Jan. 2011.
[26] Y. Zheng, H. Fang, and H. Wang, "Takagi–Sugeno fuzzy-model-based fault detection for networked control systems with Markov delays," *IEEE Trans. Syst., Man, Cybern., Part B: Cybern.*, vol. 36, no. 4, pp. 924–929, Aug. 2006.
[27] L. Zhang, Y. Shi, T. Chen, and B. Huang, "A new method for stabilization of networked control systems with random delays," *IEEE Trans. Autom. Control*, vol. 50, no. 8, pp. 1177–1181, Aug. 2005.
[28] A. Bemporad, "Predictive control of teleoperated constrained systems with unbounded communication delays," in *Proc. 37th IEEE Conf. Decision Control*, 1998, pp. 2133–2138.
[29] J. Liu, D. M. de la Peña, and P. D. Christofides, "Distributed model predictive control of nonlinear systems subject to asynchronous and delayed measurements," *Automatica*, vol. 46, no. 1, pp. 52–61, 2010.
[30] Y. Wang, S. Ding, H. Ye, and G. Wang, "A new fault detection scheme for networked control systems subject to uncertain time-varying delay," *IEEE Trans. Signal Process.*, vol. 56, no. 10, pp. 5258–5268, Oct. 2008.
[31] X. He, Z. Wang, and D. Zhou, "Robust fault detection for networked systems with communication delay and data missing," *Automatica*, vol. 45, no. 11, pp. 2634–2639, 2009.
[32] P. Zhang, S. X. Ding, G. Z. Wang, and D. H. Zhou, "Fault detection for multirate sampled-data systems with time delays," *Int. J. Control*, vol. 75, no. 18, pp. 1457–1471, 2002.
[33] H. Ye and S. Ding, "Fault detection of networked control systems with network-induced delay," in *Proc. Conf. Control Autom. Robot. Vision*, 2004, pp. 294–297.
[34] W. Qiu and R. Kumar, "Distributed diagnosis under bounded-delay communication of immediately forwarded local observations," *IEEE Trans. Syst., Man Cybern., Part A: Syst. Humans*, vol. 38, no. 3, pp. 628–643, May 2008.
[35] W. Ding, Z. Mao, B. Jiang, and W. Chen, "Fault detection for a class of nonlinear networked control systems with markov transfer delays and stochastic packet drops," *Circuits, Syst., Signal Process.*, vol. 34, no. 4, pp. 1211–1231, 2015.
[36] Y. Wang, S. Xu, and S. Zhang, "Fault detection for a class of nonlinear networked control systems with Markov sensors assignment and random transmission delays," *J. Franklin Inst.*, vol. 351, no. 10, pp. 4653–4671, 2014.
[37] J. A. Rossiter, *Model-Based Predictive Control: A Practical Approach*. Boca Raton, FL, USA: CRC Pess, 2013.
[38] L. Yan, B. Xiao, Y. Xia, and M. Fu, "The modeling and estimation of asynchronous multirate multisensor dynamic systems," in *Proc. 32nd Chinese Control Conf.*, 2013, pp. 4676–4681.
[39] P. Mhaskar, J. Liu, and P. D. Christofides, "Control and fault-handling subject to asynchronous measurements," in *Fault-Tolerant Process Control*, New York, NY, USA: Springer, 2013, pp. 205–252.
[40] F. Boem, R. M. G. Ferrari, T. Parisini, and M. M. Polycarpou, "A distributed fault detection methodology for a class of large-scale uncertain input-output discrete-time nonlinear systems," in *Proc. 50th Conf. Decision Control Eur. Control Conf.*, 2011, pp. 897–902.
[41] F. Boem, R. M. Ferrari, T. Parisini, and M. M. Polycarpou, "Optimal topology for distributed fault detection of large-scale systems," *IFAC-PapersOnLine*, vol. 48, no. 21, pp. 60–65, 2015.
[42] C. Keliris, M. M. Polycarpou, and T. Parisini, "A distributed fault detection filtering approach for a class of interconnected continuous-time nonlinear systems," *IEEE Trans. Autom. Control*, vol. 58, no. 8, pp. 2032–2047, Aug. 2013.
[43] F. Boem, R. Ferrari, T. Parisini, and M. Polycarpou, "Distributed fault detection for uncertain nonlinear systems: A network delay compensation strategy," in *Proc. 2013 Amer. Control Conf.*, 2013.
[44] P. L. Tang and C. de Silva, "Compensation for transmission delays in an ethernet-based control network using variable-horizon predictive control," *IEEE Trans. Control Syst. Technol.*, vol. 14, no. 4, pp. 707–718, Jul. 2006.
[45] J. Farrell and M. M. Polycarpou, *Adaptive Approximation Based Control: Unifying Neural, Fuzzy, and Traditional Adaptive Approximation Approaches*. Hoboken, NJ, USA: Wiley-Interscience, 2006.
[46] X. Zhang, M. M. Polycarpou, and T. Parisini, "A robust detection and isolation scheme for abrupt and incipient faults in nonlinear systems," *IEEE Trans. Autom. Control*, vol. 47, no. 4, pp. 576–593, Apr. 2002.
[47] M. M. Polycarpou, "On-line approximators for nonlinear system identification: A unified approach," in *Control and Dynamic Systems: Neural Network Systems Techniques and Applications*, X. Leondes, Ed. New York, NY, USA: Academic, 1998, vol. 7, pp. 191–230.
[48] A. Vemuri and M. M. Polycarpou, "On-line approximation methods for robust fault detection," in *Proc. 13th IFAC World Congr.*, 1996, vol. K, pp. 319–324.
[49] G. Michaletzky and L. Gerencsér, "BIBO stability of linear switching systems," *IEEE Trans. Autom. Control*, vol. 47, no. 11, pp. 1895–1898, Nov. 2002.
[50] M. L. Sichitiu and P. H. Bauer, "Stability of discrete time-varying linear delay systems and applications to network control," in *Stability and Control of Dynamical Systems With Applications*, A. Liu and P. J. Antsaklis, Eds. New York, NY, USA: Springer, Control Engineering, 2003, pp. 117–130.
[51] R. M. G. Ferrari, T. Parisini, and M. M. Polycarpou, "Distributed fault diagnosis with overlapping decompositions and consensus filters," in *Proc. Amer. Control Conf.*, 2007, pp. 693–698.
[52] M. Du and P. Mhaskar, "Isolation and handling of sensor faults in nonlinear systems," *Automatica*, vol. 50, no. 4, pp. 1066–1074, 2014.
[53] M. Du, J. Scott, and P. Mhaskar, "Actuator and sensor fault isolation of nonlinear process systems," *Chem. Eng. Sci.*, vol. 104, pp. 294–303, 2013.
[54] V. Reppa, M. M. Polycarpou, and C. G. Panayiotou, "Distributed sensor fault diagnosis for a network of interconnected cyberphysical systems," *IEEE Trans. Control Netw. Syst.*, vol. 2, no. 1, pp. 11–23, Mar. 2015.

Francesca Boem received the Laurea (M.Sc.) degree (*cum laude*) in management engineering in 2009 and the Ph.D. degree in information engineering in 2013 from the University of Trieste, Trieste, Italy

She was Post-Doctoral Researcher at the Department of Engineering and Architecture at the University of Trieste from 2013 to 2014 with the Automation Group and with the Machine Learning Group. Since 2014, she has been a Research Associate at the Department of Electrical and Electronic Engineering, Imperial College London, U.K., with the Control and Power Research Group. She cooperated with the R&D department of Danieli Automation SpA, Buttrio (UD), Italy. She has authored and coauthored several papers published in international journals and conference proceedings. Her current research interests include distributed fault-diagnosis methods for large-scale networked systems and distributed estimation methods for sensor networks. She is reviewer for various conferences and journals.

Riccardo M. G. Ferrari received the Laurea degree (cum laude and printing honours) in electronic engineering in 2004 and the Ph.D. degree in information engineering in 2009, both from the University of Trieste, Trieste, Italy.

He has authored and coauthored over 19 papers published in international peer-reviewed journals and conference proceedings. He has covered a unique career path that led him to hold both academical and industrial R&D positions, in particular as Researcher and Executive Manager in the field of process instrumentation and control for the steelmaking sector. He is now a Post-Doctoral Research Fellow at the Delft University of Technology, Delft, The Netherlands, in the Delft Center for Sytems and Control. His research interests include fault diagnosis, nonlinear distributed systems, smart buildings and HVAC, numerical modelling, and industrial applications of advanced monitoring and control techniques.

Dr. Ferrari is the recipient of the 2005 Giacomini Award of the Italian Acoustic Society.

Christodoulos Keliris (M'15) received the diploma degree in electrical and computer engineering (Hons.) from the Aristotle University of Thessaloniki, Thessaloniki, Greece, in 2007, the M.Sc. degree in finance (Hons.) from Imperial College London, London, U.K., in 2008, and the Ph.D. degree in electrical engineering from the University of Cyprus, Nicosia, Cyprus in 2015. His dissertation Pricing barrier options was awarded the Best M.Sc. Finance Dissertation prize.

He was a Researcher in various European research and operational programs. His research interests include fault diagnosis for nonlinear systems, nonlinear control theory, adaptive learning, and intelligent systems.

Dr. Keliris is a reviewer for various conferences and journals.

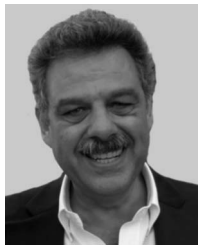

Thomas Parisini (F'11) holds the Chair of Industrial Control and is Director of Research at Imperial College London, London, U.K. Since 2001 he has also been the Danieli Endowed Chair of Automation Engineering with University of Trieste, Triest, Italy. He was with Politecnico di Milano, Italy. He has authored or coauthored more than 270 research papers in archival journals, book chapters, and international conference proceedings. His research interests include neural-network approximations for optimal control problems, fault diagnosis for nonlinear and distributed systems, nonlinear model predictive control systems, and nonlinear estimation.

Dr. Parisini is a corecipient of the IFAC Best Application Paper Prize of the Journal of Process Control, Elsevier, for the three-year period 2011–2013 and of the 2004 Outstanding Paper Award of the IEEE TRANSACTIONS ON NEURAL NETWORKS. He is the Editor-in-Chief of the IEEE TRANSACTIONS ON CONTROL SYSTEMS TECHNOLOGY, and he is the Chair of the IFAC Technical Committee on Fault Detection, Supervision and Safety of Technical Processes "SAFEPROCESS." In 2012 he was awarded a prestigious ABB Research Grant dealing with energy-autonomous sensor networks for self-monitoring industrial environments.

Marios M. Polycarpou (F'06) received undergraduate degrees in computer science and in electrical engineering, both from Rice University, Houston, TX, USA in 1987, and the M.S. and Ph.D. degrees in electrical engineering from the University of Southern California, Los Angeles, CA, USA, in 1989 and 1992 respectively.

He is a Professor of electrical and computer engineering and the Director of the KIOS Research Center for Intelligent Systems and Networks at the University of Cyprus, Nicosia, Cyprus. His teaching and research interests are in intelligent systems and networks, adaptive and cooperative control systems, computational intelligence, fault diagnosis, and distributed agents. He has published more than 280 articles in refereed journals, edited books and refereed conference proceedings, and coauthored 7 books. He is also the holder of 6 patents.

Prof. Polycarpou has served as the President of the IEEE Computational Intelligence Society (2012–2013). He has served as the Editor-in-Chief of the IEEE TRANSACTIONS ON NEURAL NETWORKS AND LEARNING SYSTEMS between 2004–2010. He is the recipient of the IEEE Neural Networks Pioneer Award for 2016. He has participated in more than 60 research projects/grants, funded by several agencies and industry in Europe and the U.S., including the prestigious European Research Council (ERC) Advanced Grant.